




# Phanerozoic low-temperature evolution of the Uruguayan Shield along the South American passive margin

Mathias Hueck<sup>1\*</sup>, Sebastián Oriolo<sup>1</sup>, István Dunkl<sup>1</sup>, Klaus Wemmer<sup>1</sup>, Pedro Oyhantçabal<sup>2</sup>, Max Schanofski<sup>1</sup>, Miguel Ângelo Stipp Basei<sup>3</sup> & Siegfried Siegesmund<sup>1</sup>

<sup>1</sup> Geoscience Centre, Georg-August-Universität Göttingen, Göttingen, Germany

<sup>2</sup> Departamento de Geología, Facultad de Ciencias, Universidad de la República, Montevideo, Uruguay

<sup>3</sup> Instituto de Geociências, Universidade de São Paulo, São Paulo, Brazil

 K.W., 0000-0002-7818-5135; M.A.S.B., 0000-0002-3857-7089; S.S., 0000-0002-5382-0622

\* Correspondence: [mathiashueck@gmail.com](mailto:mathiashueck@gmail.com)

**Abstract:** The crystalline basement of Uruguay was assembled during the Brasiliano Orogeny in the Neoproterozoic Era and was later affected by discrete tectonic activity. A new multi-method low-temperature dataset including (U–Th)/He ages from both zircon and apatite,  $T-t$  modelling and K–Ar dating of fine sericite fractions and fault gouge reveal a detailed post-orogenic geological history spanning the Phanerozoic Eon. The juxtaposition of the terranes that compose the area was achieved in the Ediacaran Period, and post-collision was marked by intense exhumation, in which the crystalline basement reached near-surface conditions by the early to mid-Palaeozoic. Regional subsidence promoted sedimentation in the Paraná Basin until the Permian, covering and reheating much of the basement that is at present exposed. Afterwards, deposition and volcanism were mostly confined to its current limits. Regional exhumation of the shield during the Permo-Triassic exposed much of the northern portion of the basement, and the south was further affected by the opening of the South Atlantic Ocean during the Mesozoic. Little exhumation affected the Uruguayan Shield during the Cenozoic, as reflected in its modest topography. The reactivation of inherited Neoproterozoic structures influenced the development of Mesozoic basins and the present-day landscape.

**Supplementary material:** Supplementary data (sample locations, (U–Th)/He data and K–Ar data) are available at <https://doi.org/10.6084/m9.figshare.c.3702043>

**Received** 2 August 2016; **revised** 10 January 2017; **accepted** 13 January 2017

The eastern coast of the South American continent has long been the subject of thermochronology studies, which have focused on the rift and post-rift evolution of its ‘passive’ margin, and especially on its steep coastal ranges (e.g. Tello Saenz *et al.* 2003; Hackspacher *et al.* 2004; Franco-Magalhães *et al.* 2010, 2014; Cogné *et al.* 2011, 2012; Karl *et al.* 2013; Jelinek *et al.* 2014). Older ages recording pre-rift exhumation, however, are usually restricted to a few samples that were not as strongly overprinted by the intense uplift during the Cretaceous Period and Cenozoic Era (Hiruma *et al.* 2010; Karl *et al.* 2013; Jelinek *et al.* 2014).

There is, however, evidence of the influence of far-reaching tectonic processes from the Gondwanan active margin into the interior part of the supercontinent, as recorded in its long sedimentary history (Zalán *et al.* 1990; López-Gamundi & Rossello 1993; Zeffass *et al.* 2004; Milani *et al.* 2007). With the recent extension of the low-temperature investigations to study areas less affected by the rift and post-rift uplift, this complex history is now being identified in the thermochronological record (Kollenz 2015; Oliveira *et al.* 2015).

One such area is the crystalline basement of Uruguay, which occupies much of the south and east of the country. It is an association of Precambrian tectonic terranes assembled during the Neoproterozoic Brasiliano Orogeny, covered by a large intracratonic basin and disrupted by the onset of an aborted rift during the South Atlantic opening (de Santa Ana *et al.* 2006; Rossello *et al.* 2007; Oyhantçabal *et al.* 2011a; Rapela *et al.* 2011; Oriolo *et al.* 2016a).

In this paper we present a multi-method low-temperature study of the Uruguayan Shield, combining (U–Th)/He ages from both zircon

and apatite,  $T-t$  modelling and K–Ar dating of fine sericite fractions and fault gouge clays. The results reveal a protracted exhumation history spanning almost the entire Phanerozoic, from the post-collisional phase of the Brasiliano Orogeny to the rifting of the South Atlantic Ocean. The new data are discussed considering the sedimentary and geomorphological record in the area, and are compared with the few local pre-existing low-temperature data and regional constraints. Furthermore, we address the influence of the inherited structural framework after the end of the orogenic process and during the sedimentary evolution of the area in light of the new data.

## Geological overview

### Crystalline basement

The Uruguayan Shield is located in SE South America along the Atlantic Ocean margin and the Rio de la Plata estuary. It is composed of rocks ranging in age from Archaean to Neoproterozoic, which are cross-cut by regional shear zones, and is limited to the north and west by the Palaeozoic to Mesozoic sediments of the Paraná Basin (locally referred to as the Norte Basin). Traditionally, it has been divided into three domains: the Piedra Alta and Nico Pérez terranes and the Dom Feliciano Belt (Fig. 1).

The Dom Feliciano Belt extends for about 1400 km from south Brazil to Uruguay, comprising the southern termination of the Mantiqueira Province (Almeida *et al.* 1981). It represents the result of the tectonic juxtaposition of several crustal blocks during the Brasiliano–Pan-African Orogeny, culminating in the consolidation

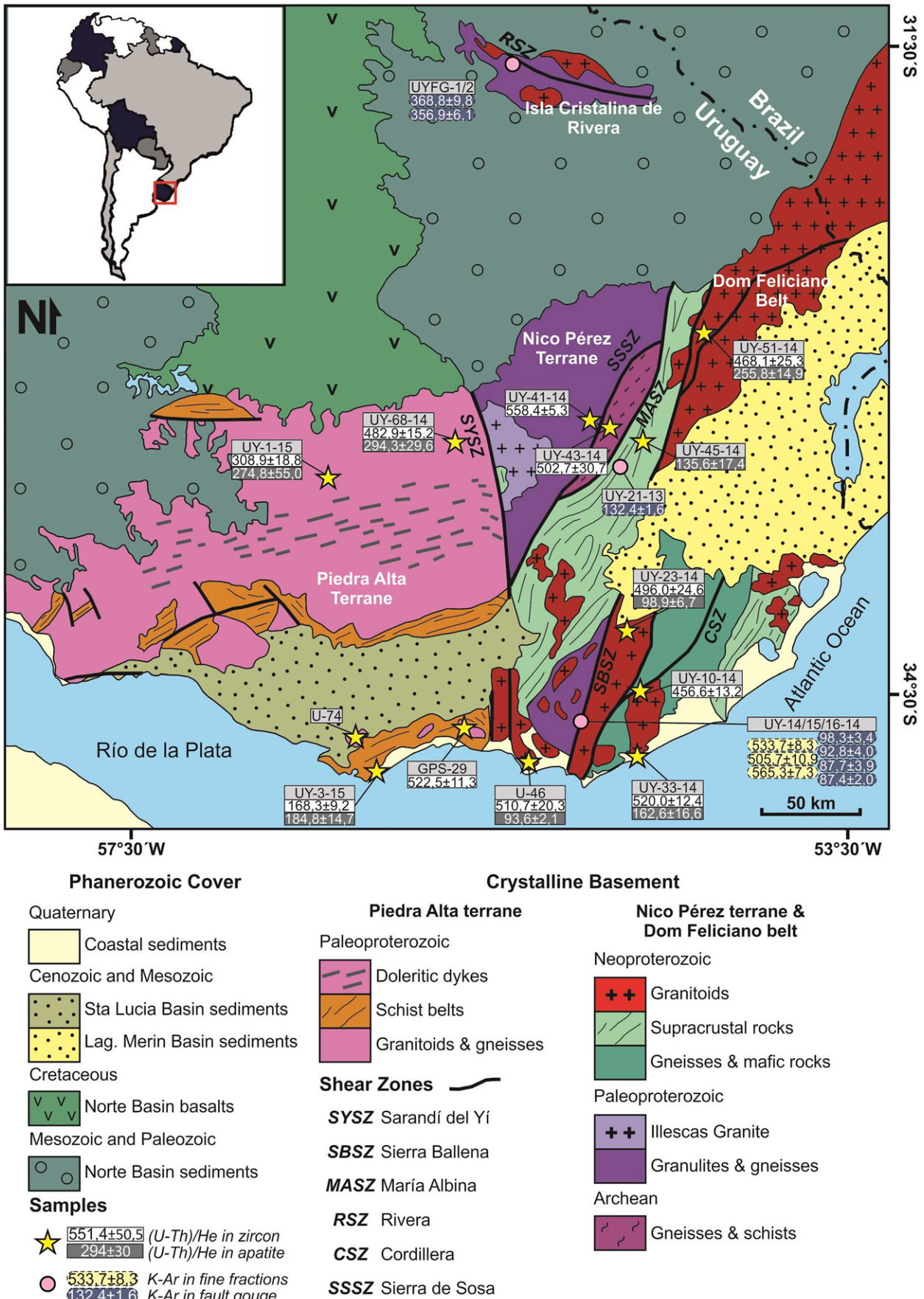


Fig. 1. Geological map of the Uruguayan Shield with sample localities and (U-Th)/He and K-Ar results. Modified after Sánchez Bettucci *et al.* (2010), Oyhançabal *et al.* (2011a) and Oriolo *et al.* (2015).

of West Gondwana. From east to west, the Dom Feliciano Belt is divided into three domains: the Granite Belt, Schist Belt and foreland basins (Basei *et al.* 2000).

In Uruguay, the Granite Belt is represented by the Aiguá Batholith, which correlates with the Brazilian Pelotas and Florianópolis Batholiths, all of which comprise intrusions with emplacement ages between 650 and 560 Ma (e.g. Philipp & Machado 2005; Oyhantçabal *et al.* 2009a; Chemale *et al.* 2012; Florisbal *et al.* 2012). These intrusions are usually related to shear zones, resulting in rocks with variable amount of strain (Bitencourt & Nardi 2000; Oyhantçabal *et al.* 2009a, 2011b; Passarelli *et al.* 2010). The Schist Belt, an association of deformed volcano-sedimentary rocks metamorphosed under greenschist- to amphibolite-facies conditions, corresponds in Uruguay to the Lavalleja Group, and is correlated in Brazil to the Brusque and Porongos groups (e.g. Basei *et al.* 2008). The Uruguayan foreland basin differs from its Brazilian counterparts (Itajaí and Camaquã basins) in being relatively thin and discontinuous, thus being separated into different stratigraphic units with unclear correlations (Basei *et al.* 2000).

The Sierra Ballena Shear Zone separates the Granite Belt from the Schist Belt, and is associated with several smaller transpressive structures on both sides, such as the Cordillera Shear Zone. Its evolution records two main shearing periods, the first around 630–600 Ma and responsible for nucleation of the vertical shear zones, whereas the second sinistral event reactivated the structure and created the present geotectonic configuration between 600 and 580 Ma (Oyhantçabal *et al.* 2009a; Oriolo *et al.* 2016b). Pre-Brasiliano basement inliers are present on both sides of the structure; namely, the Campanero Unit in the west and the Cerro Olivo Complex in the east (Sánchez Bettucci *et al.* 2004; Oyhantçabal 2005; Mallmann *et al.* 2007; Oyhantçabal *et al.* 2009b; Basei *et al.* 2011; Lenz *et al.* 2011).

The main unit in the Nico Pérez Terrane is the Valentines–Rivera Complex, an assemblage of Palaeoproterozoic gneiss and granulite that extends through the Isla Cristalina de Rivera region and connects to the Santa Maria Chico Complex in the Brazilian Taquarém Block (Hartmann *et al.* 2008; Oyhantçabal *et al.* 2011a, 2012; Oriolo *et al.* 2016a). It is intruded on its western border by the large Statherian Illescas Rapakivi Granite (Campal & Schipilov 1995), whereas on the east it is juxtaposed by means of the Sierra de Sosa Shear Zone to the La Chinas Complex, an Archaean block consisting of metamorphosed mafic to ultramafic rocks and gneisses (Hartmann *et al.* 2001; Oyhantçabal *et al.* 2011a). During the Neoproterozoic, the Nico Pérez Terrane was intensely reworked by its interaction with the Dom Feliciano Belt, as evidenced by regional K–Ar cooling ages, widespread granitic magmatism and the development of several internal shear zones, such as the Maria Albina Shear Zone and Rivera Shear Zone (Oyhantçabal *et al.* 2007, 2011a, 2012; Oriolo *et al.* 2015, 2016b,c).

In the westernmost area of the shield, the Piedra Alta Terrane is dominated by a Palaeoproterozoic association that comprises a large granitic–gneiss area associated with metavolcano-sedimentary belts, which were in turn intruded by late- to post-tectonic granitic intrusions (Oyhantçabal *et al.* 2011b). This domain is correlated with the Tandilia Belt in Argentina (Cingolani 2011), forming the Rio de la Plata Craton (Almeida *et al.* 1973). This tectonic unit is largely covered by Phanerozoic sediments and thus most of its margins are concealed, but in Uruguay its eastern border to the Nico Pérez Terrane is well characterized by the Sarandí del Yí Shear Zone (Oyhantçabal *et al.* 2011a; Rapela *et al.* 2011; Oriolo *et al.* 2015, 2016c). As with the Sierra Ballena Shear Zone, the Sarandí del Yí Shear Zone has a long Neoproterozoic deformational history. It began with an early dextral shear under middle to upper amphibolite metamorphic conditions and subsequent sinistral shear under lower amphibolite to upper greenschist conditions, followed by late cataclastic reactivations (Oriolo *et al.* 2015, 2016c).

### *Sedimentary record*

Around half of the territory of Uruguay is covered by the Paraná Basin, which is locally known as the Norte Basin. This major intracratonic basin covers around 1.5 million km<sup>2</sup>, spreading into Brazil, Paraguay and Argentina, and was deposited in the Palaeozoic and Mesozoic eras. Although a total thickness of more than 6 km is assumed for the whole depositional assembly (Zalán *et al.* 1990), in eastern Uruguay it does not exceed 2.5 km, owing to its marginal position (de Santa Ana 2004).

The main Palaeozoic sedimentation consists of two transgressive–regressive cycles. The first corresponds to the Devonian Durazno Group, has a thickness of less than 300 m (Uriz *et al.* 2016) and is part of the Paraná Supersequence within the stratigraphic framework of the regional basin (Milani *et al.* 2007). The second succession, deposited during the Permian and early Triassic periods, encompasses the Cerro Largo Group (de Santa Ana *et al.* 2006), which, with over 1000 m of sediments, is associated with the larger Gondwana I Supersequence (Milani *et al.* 2007).

Regional stratigraphic unconformities and sedimentation gaps are observed at the top of both Palaeozoic sequences, leading some researchers to propose periods of uplifting regimes linked to the influence of orogenic cycles in the borders of Gondwana (Zalán *et al.* 1990; López-Gamundi & Rossello 1993; de Santa Ana 2004). Sedimentation in the Paraná Basin was limited in middle and late Triassic times to extensional basins of local extent mostly restricted to southern Brazil, collectively referred to as the Gondwana II Supersequence (Zerfass *et al.* 2004; Milani *et al.* 2007).

The last sedimentary association in the Uruguayan portion of the Paraná Basin, linked to the Gondwana III Supersequence (Milani *et al.* 2007), consists of continental sediments capped by massive volcanic flows exceeding 1000 m in thickness. This extraordinary extrusive event is associated with the break-up of the Pangaea supercontinent and the opening of the South Atlantic Ocean, and dates to the early Cretaceous, between 135 and 130 Ma (Renne *et al.* 1992; Janasi *et al.* 2011).

During this event, the Neoproterozoic configuration of the Uruguayan Shield was disrupted by the installation of a rift corridor along the Santa Lucia–Aiguá–Merin Lineament (Rossello *et al.* 2000, 2007), which culminated in the onset of two pull-apart basins: the Laguna Merin in the NE and Santa Lucia in the SW. The former is c. 2000 m thick and has a predominantly sedimentary infill, whereas the latter comprises up to a thousand metres of basaltic rocks coeval with the Paraná lava flows, later intruded by gabbro and trachyte complexes (Cernuschi *et al.* 2015).

According to Rossello *et al.* (2000, 2007), the Santa Lucia–Aiguá–Merin Lineament began as an aborted rift during the opening of the South Atlantic Ocean and developed into a dextral transcurrent corridor, which helped expand the basins. The same researchers pointed to the influence of Brasiliano-related structures on the lineament. Although the Santa Lucia–Aiguá–Merin Lineament cuts through shear zones of the crystalline basement in Uruguay, the boundaries of both basins are determined by the Sierra Ballena Shear Zone and the Sarandí del Yí Shear Zone, creating a central domain in which only vestiges of the volcano-sedimentary infill are preserved.

Deposition along the Santa Lucia–Aiguá–Merin Lineament corridor lasted throughout the Cenozoic, a period during which most of Uruguay was affected by uplift and erosion (Panario *et al.* 2014). Thus, the continental sedimentary record of this period is mostly confined to that corridor. Nonetheless, the opening of the South Atlantic Ocean marked the setting of sedimentary basins on South America's continental margins, characterized by a succession of offshore deposits separated by structural highs. The continental margin basins of Uruguay present a thickness of over 8 km based on seismic data and reach more than 300 km away from the coast (Soto

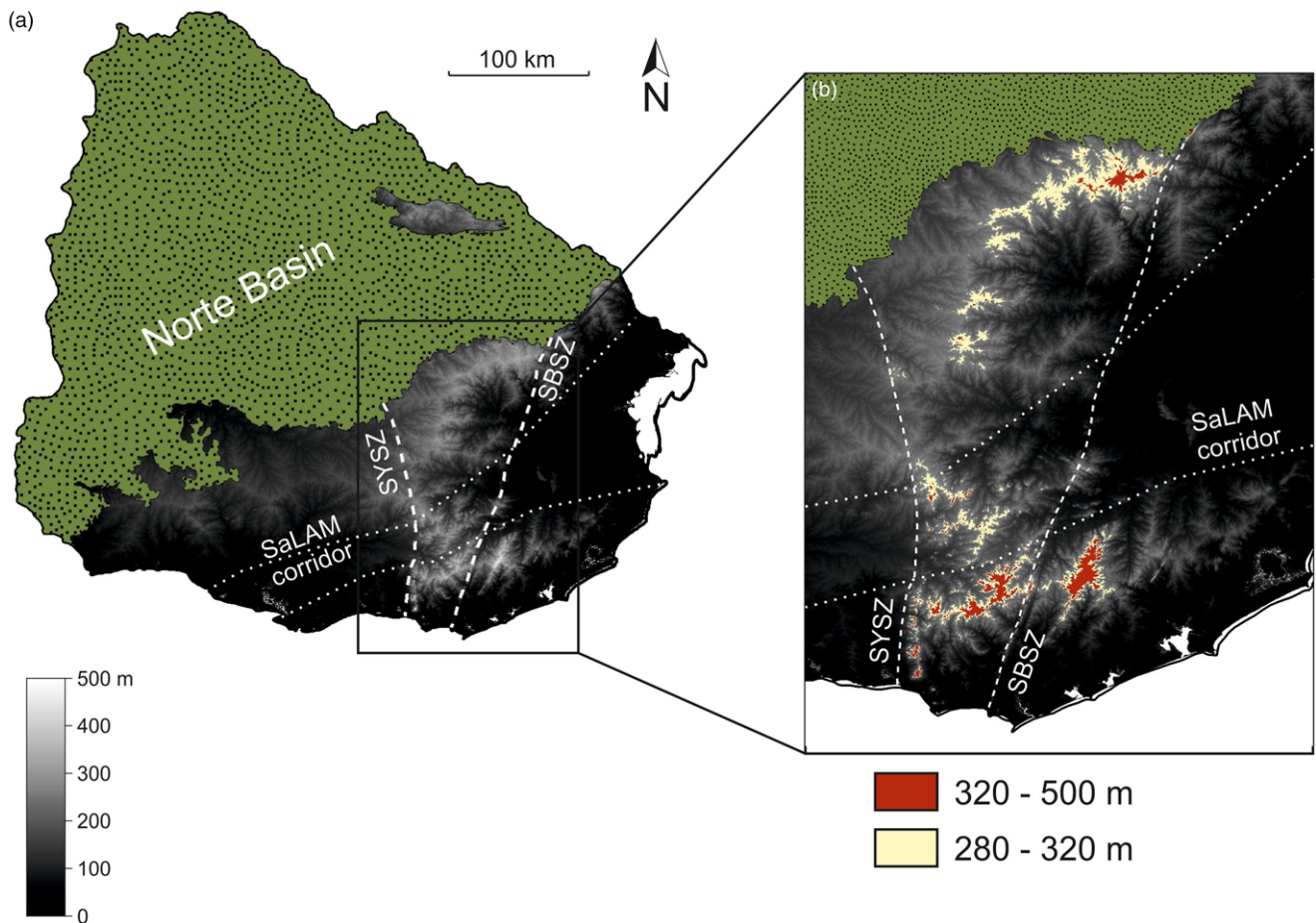


**Fig. 2.** Digital elevation model of the Uruguayan Shield (a) with indication of the shear zones that separate the main terranes and detail of the extent of the main palaeosurfaces (b).

*et al.* 2011). They encompass part of the Pelotas and Punta del Este basins as well as a third, distal one called Oriental del Plata.

### Geomorphological aspects

The Uruguayan Shield is generally flat and its modest ranges hardly exceed 500 m in altitude, thus differing from the passive Atlantic margin further north in south and SE Brazil, in which the highest peaks exceed 2000 m. The most elevated areas within Uruguay form a watershed dividing the country with an approximate north–south orientation, and were referred to as the geomorphological Eastern Hills Region by Panario *et al.* (2014).

Geologically, these areas correspond to rocks associated with the Dom Feliciano Belt and the Nico Pérez Terrane. Its prominence is especially accentuated in the southern portion of Uruguay, between the Santa Lucia–Aiguá–Merin Lineament and the coastal shoreline. With the notable exception of the Carapé Massif, a part of the Granitic Belt that sustains the culminating peak in the country (Cerro Catedral), this topographically elevated domain is almost entirely bound to the east by the Sierra Ballena Shear Zone and to the west by the Sarandí del Yí Shear Zone (Fig. 2a). An extreme example of the topographic contrast along the Nico Pérez Terrane, enhanced by differential erosion caused by lithological differences, is the western flank of the Sierra de las Animas located in the southern extent of the Sarandí del Yí Shear Zone (Fig. 3a). This contrast, however, is not uniform along the length of the structure.

Restricted vestiges of elevated palaeosurfaces occur in the Eastern Hills Region. Panario *et al.* (2014) identified two distinct levels (Fig. 2b). The upper surface comprises elevations between 320 and 500 m and is particularly well exposed where flat

weathering fronts have been preserved on the Cerro Catedral (Fig. 3b). The lower palaeosurface, situated between 280 and 320 m and exposed in such ranges as the Aiguá and Yerbál Sierras, displays better developed soil horizons (Fig. 3c,d). Both surfaces were interpreted to have a Mesozoic origin by Panario *et al.* (2014), and correlate well with the geomorphology of the coastal Tandilia range in the Argentinian portion of the Rio de la Plata Craton (Demoulin *et al.* 2005).

### Methods

#### Sampling

Sampling for the (U–Th)/He method focused mostly on granitoids and gneisses. A total of 29 samples were selected for mineral concentration following standard density and magnetic separation techniques. Eleven samples were selected for zircon analysis and nine for apatite, comprising all of the main tectonic blocks on the Uruguayan Shield. Seven of these samples yielded both minerals, with the potential to reveal more detailed thermal paths during modelling.

Fault gouge samples were collected in outcrops associated with significant shear zones of the crystalline basement. When possible, duplicates of gouge material exhibiting different aspects on a same fault were collected to obtain age controls. The sampled fault gouge along the Sierra Ballena Shear Zone has a thickness of several tens of centimetres and is composed of yellow clay without lithic fragments. The main mineral is kaolinite, with subsidiary proportions of illite. The fault gouge associated with the Maria Albina Shear zone is less than 10 cm thick and is composed of slightly

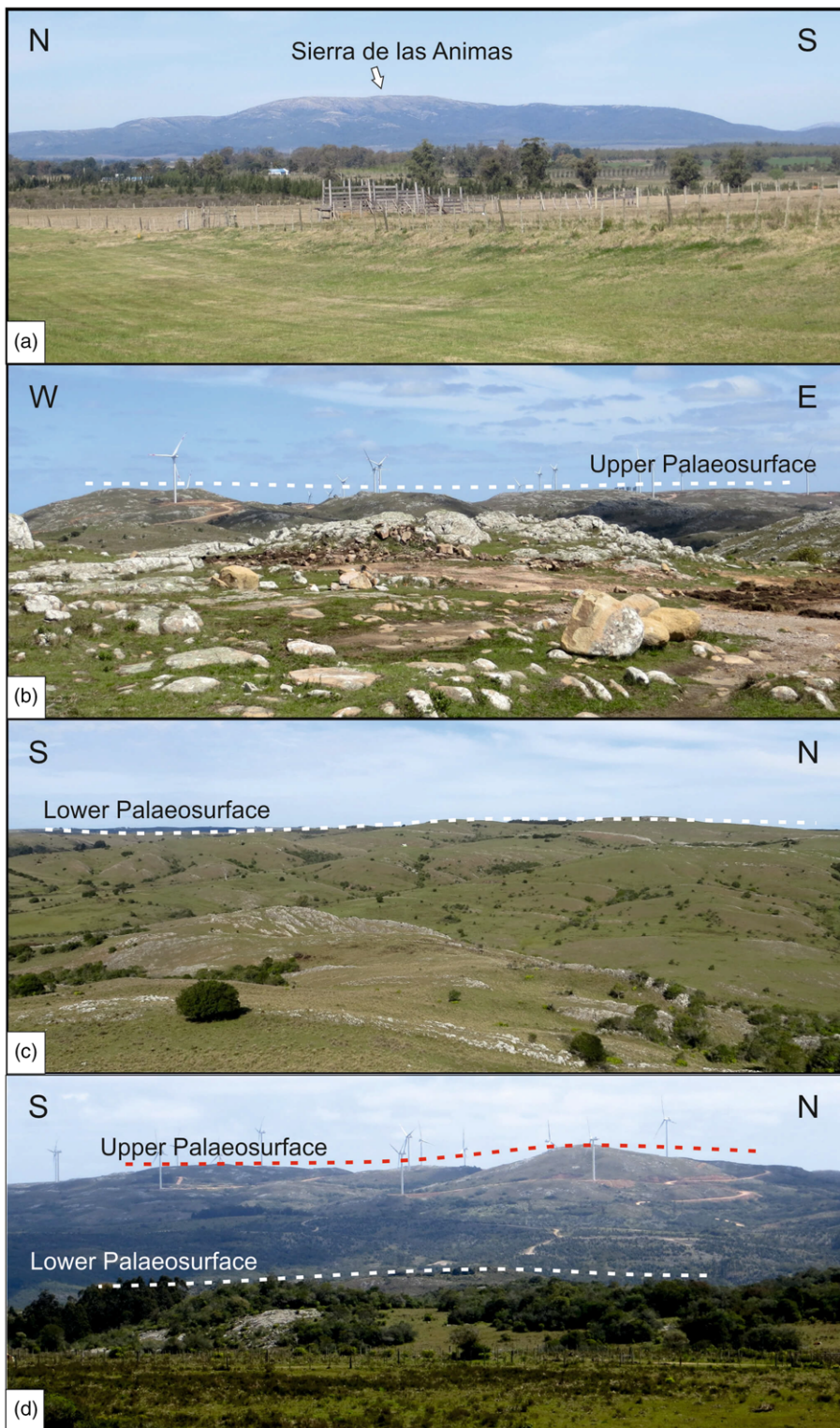


**Fig. 3.** Typical landscapes of the Uruguayan Shield: (a) strong topographic contrast on the western flank of the Sierra de las Animas, along the Sarandi del Yi Shear Zone; (b) upper palaeosurface visible as flat hilltops close to the Cerro Catedral (elevation *c.* 480 m); (c) lower planation surface, strongly dissected with the formation of valleys along main drainage paths (elevation *c.* 280 m); (d) view to the upper palaeosurface from the lower palaeosurface (elevation *c.* 310 m).

textured dark grey clay. Again, illite occurs as an accessory for a material mostly composed of kaolinite. The samples associated with the Rivera Shear Zone were collected on a gouge less than 1 cm thick, light grey to green in colour and with abundant lithic fragments. All sampled faults were parallel to host rock foliation and to the direction of the shear zones. Fine fractions of sericite extracted from the mylonitic host rock alongside the sampled gouge in the Sierra Ballena Shear Zone were also dated by K–Ar to estimate the age of the brittle–ductile transition in the shear zone. The coordinates of all analysed samples are presented in the Supplementary Material, and their location is shown in Figure 1.

### *Zircon and apatite (U–Th)/He thermochronology*

Three single-crystal aliquots were handpicked from the selected samples using a stereomicroscope and a polarizing microscope. Only euhedral, clear, inclusion- and fissure-free crystals with a minimum diameter of 60 µm were selected, preferentially with presence of both pyramidal terminations. Each mineral was photographed, and the images were used for determining crystal length, width and prismatic length. These parameters were used for correcting for alpha-particle ejection, as discussed by Farley *et al.* (1996).

For the extraction of helium the zircon and apatite crystals were wrapped in platinum capsules and heated in a high vacuum with an infrared laser. The extracted gas was purified with an SAES Ti–Zr getter operating at 450°C, and the remaining inert gases were measured in a Hitachi triple-filter quadrupole mass spectrometer equipped with a positive ion-counting detector. To control the efficiency of the gas extraction, a re-extraction was performed for each crystal.

After degassing, the crystals were retrieved from the capsules and spiked with  $^{230}\text{Th}$  and  $^{233}\text{U}$  solutions before being dissolved using distilled 48% HF + 65% HNO<sub>3</sub> for 5 days in pressurized Teflon bombs at 220°C, in the case of zircon, and 2% HNO<sub>3</sub> at room temperature in an ultrasonic bath for apatite. The measurement of the radioactive elements (U, Th and Sm) in the spiked solutions was conducted by inductively coupled plasma mass spectrometry (ICP-MS) using a Perkin Elmer Elan DRC II system equipped with an APEX MicroFlow nebulizer, by the isotope dilution method. Analytical data were reduced and the ages were calculated by MASsoft (software of the mass spectrometer) and the PEPITA freeware (Dunkl *et al.* 2008).

### Modelling the temperature history

Cooling trajectories were modelled using HeFTY 1.8.3 software (Ketcham 2005) for every sample in which both zircon and apatite (U–Th)/He ages were obtained. Results from samples UY-43-14 and UY-45-14 were modelled together, assuming a combined geological evolution. Calibration models for zircon (Guenther *et al.* 2013) and apatite (Flowers *et al.* 2009) considered U, Th and Sm concentrations for every crystal, as well as their dimensions. Within the model, calculated ages were corrected for alpha ejection age according to Ketcham *et al.* (2011). Obtained fits were categorized as either good or acceptable matches, according to general recommendations by Ketcham (2005). Samples were modelled using all measured crystals, but results failing to produce acceptable fits were recalculated on the basis of only two crystals of each mineral.

Initially, all samples went through an unsupervised model, in which only starting and ending points were fixed. Regional muscovite cooling ages were represented by a time–temperature constraint at 350–425°C (after Purdy & Jäger 1976, and Harrison *et al.* 2009), centred at 600 Ma for basement units and of 580 Ma for Dom Feliciano Belt granitic intrusions (Oyhantçabal *et al.* 2009b; Oriolo *et al.* 2016b), and annual mean surface temperatures of  $17 \pm 2^\circ\text{C}$  were assumed. For samples of the Piedra Alta Terrane, in which muscovite cooling ages are Palaeoproterozoic (Oyhantçabal *et al.* 2011a), a temperature interval was fixed shortly before the oldest single-crystal ZHe age at 160–200°C, beyond the limit of the ZHe method.

Following this first approach, each sample was tested for a set of four independent hypotheses, based on the sedimentary record covering the Uruguayan Shield. Hypothesis 1 assumes an exhumation shortly after the Brasiliano Orogeny and predating the first Phanerozoic sediments in the Norte Basin; that is, the Devonian Durazno Group (part of the Paraná Sequence after Milani *et al.* 2007). This scenario was modelled by fixing time–temperature constraints for the modelling below 60°C during the 440–420 Ma interval, in the Silurian Period. The reburial event caused by the Palaeozoic sedimentation of the Paraná Basin did not exceed 90°C, a value independently provided by organic maturation data determined close to the study area (Silva & Cornford 1985). This estimation also considers the strong likelihood of sample locations at the edge of the basin, and assumes that the basement was little affected by the intrusion of basic rocks associated with the Cretaceous magmatism, which was responsible for the most intense maturations recorded in this sequence (Zalán *et al.* 1990; Hurter & Pollack 1994; Souza *et al.* 2008). Hypothesis 2 postulates a similar exhumation with exposure to surface conditions after the

**Table 1.** Summary of the hypotheses tested during thermal modelling

Hypothesis	Assumption	Constraints
1	Currently exposed basement surface was at a shallow crustal depth during the Silurian before subsequent burial followed by exhumation	Temperatures below 60°C c. 440–420 Ma, reburial event did not exceed 90°C
2	Currently exposed basement surface was at a shallow crustal depth during the Devonian–Carboniferous before subsequent burial followed by exhumation	Temperatures below 60°C c. 420–320 Ma, reburial event did not exceed 90°C
3	Currently exposed basement surface was at a shallow crustal depth during the Jurassic before subsequent burial followed by exhumation	Temperatures below 60°C c. 200–160 Ma, reheating event did not exceed the detection limits of the (U–Th)/He method
4	Currently exposed basement never experienced surface conditions prior to the (U–Th)/He cooling ages	Temperatures above 60°C prior to the (U–Th)/He cooling ages

Brasiliano Orogeny, during or after the Devonian sedimentation, but before the onset of Permian Gondwana I deposition in the Norte Basin (Milani *et al.* 2007). This hypothesis would allow the sampled area to act as a possible provenance source for the Durazno Group as postulated by Uriz *et al.* (2016), and was modelled by placing a time–temperature constraint below 60°C during the Devonian and early Carboniferous periods (420–320 Ma). As with Hypothesis 1, the maximum temperature assumed as a result of the Palaeozoic deposition was 90°C. Hypothesis 3 adopts an exposure to surface conditions during the early and middle Jurassic, shortly before the onset of the Paraná volcanism. This was constrained by means of a time–temperature constraint below 60°C from 200 to 160 Ma. The maximum temperature associated with the reheating events was limited only by the thermal limits of the (U–Th)/He method, as it is entirely dependent on the effect of the volcanic rocks. Furthermore, this hypothesis was rejected for samples UY-68-14 and UY-51-14, which provide AHe ages older than the Jurassic Period. Lastly, Hypothesis 4 works under the assumption that the sampled rocks were never exposed to near-surface conditions prior to their apparent AHe age. This was constrained by preventing the tested thermal trajectories from reaching temperatures below 60°C before the AHe apparent age. The hypotheses described above are summarized in Table 1.

All samples were tested for 100 000 independent trajectories, or until the 100th good fit. With the exception of the constraints determining the age of exhumation, the configuration of the models was kept as similar as possible for all hypotheses to minimize the effect in the obtained results of variations of the tested areas of the diagrams. It should also be noted that although Hypotheses 1–3 fix a determined period in which the sample was close to the surface, the modelling was unconstrained and allowed additional exhumation and burial events in other time intervals.

Sample UY-1-15 could not be tested for these four hypotheses because, unlike the other samples, its ZHe and AHe error margins overlap. This implies a rather straightforward thermal history, which was therefore calculated by using the simple unconstrained model.

### K–Ar in fault gouge and fine fractions

K–Ar dating of illite-bearing fault gouge can be used for determining the age of brittle faulting events (e.g. van der Pluijm *et al.* 2001; Haines & van der Pluijm 2008; Zwingmann *et al.* 2010;

Bense *et al.* 2014; Ksienzyk *et al.* 2016), and its use combined with other geochronological and structural methods is becoming more frequent (e.g. Löbens *et al.* 2011; Tagami 2012; Wolff *et al.* 2012; Fossen *et al.* 2016).

About 200 g from each sample of fault gouge or of pulverized rock (in the case of fine-fraction dating) were sieved after being dispersed in water. Three grain-size fractions were extracted and measured for each sample: 2–6  $\mu\text{m}$ , <2  $\mu\text{m}$  and <0.2  $\mu\text{m}$ . The first two fractions were obtained by means of differential settling in water using the Atterberg method, whereas the latter was enriched using ultra-centrifugation.

X-ray diffraction (XRD) analyses on both randomly oriented samples and oriented (textured) compounds were used to identify the mineralogy of the fault gouge samples using a Phillips PW 1800 X-ray diffractometer. Potassium and argon were measured independently. The Ar isotopic concentrations were obtained with an Argus VI (Thermo Fisher) noble-gas mass spectrometer coupled to a glass extraction and purification vacuum line. Extraction was performed by fusing the samples after they were pre-heated to reduce the amount of atmospheric argon adsorbed to the mineral surfaces. Radiogenic  $^{40}\text{Ar}$  concentrations were determined by the isotope dilution method using an enriched  $^{38}\text{Ar}$  spike (Schumacher 1975). The spike was calibrated against the HD-B1 biotite standard (Fuhrmann *et al.* 1987). Flame photometry was used to determine the amount of K in samples dissolved in a mixture of HF and  $\text{HNO}_3$  using a BWB-XP flame photometer. The analytical error for the K–Ar age calculations is given at a 95% confidence level ( $2\sigma$ ). Data reproducibility was tested by dating two independent samples from the Sierra Ballena Shear Zone twice. Further information on the GZG K–Ar laboratory routine has been provided by Wemmer (1991).

## Results of helium thermochronology

### Zircon (U–Th)/He ages

Zircon (U–Th)/He ages (ZHe) are presented in Figure 1, and the analytical data are available in the Supplementary Material. A few outlier ages were discarded as unrealistic within the regional context; these ages were probably biased by high radiation damage density and the strong core–rim zoning of the actinide elements. These results were not considered for the calculation of average ages and are not reported in the following sections. Additional analyses using Raman spectroscopy of zircons from a discarded sample indicated a low degree of ‘crystallinity’, probably caused by the accumulated radiation damage (e.g. Nasdala *et al.* 2001).

Nonetheless, the effect of radiation damage is of little consequence to crystal analysis. Effective uranium content (eU) values are wide-ranging, with most crystals having values between 30 and 600 ppm. Samples with older stratigraphic ages occasionally have more elevated eU values. There is, however, no evident intra-sample correlation pattern between the obtained ZHe ages and either eU or crystal size, and even samples from the same domain that yielded similar ages have different and non-linear patterns. This behaviour unfortunately prevents any attempt to further enhance thermal modelling by applying eU as a criterion (e.g. Guenther *et al.* 2015; Orme *et al.* 2016).

The samples’ average ZHe ages are consistent throughout the Uruguayan Shield (Fig. 1), covering an interval of *c.* 100 myr (560–460 Ma); that is, from the end of the Ediacaran to the Ordovician. These ages extend continuously throughout this time span, not converging to any given episode. The only exception is sample UY-1-15, collected in the interior part of the Piedra Alta Terrane. It produced an age of  $309 \pm 19$  Ma, which is almost 150 myr younger than the time interval set by the remaining samples.

Concerning the obtained ages, with the exception of sample UY-1-15, no regional trend is discernible, not even along the main Brasiliano shear zones. Relatively old ages occur close to young ones, and even the most significant geological structures may lie between samples displaying age differences of only 10 or 20 myr, such as in the southern part of the study area. The oldest recorded age ( $558 \pm 5$  Ma) was obtained in a gneiss sample from the granulitic basement of the Nico Pérez Terrane, whereas the youngest ( $457 \pm 13$  Ma) comes from mylonitic rocks along the Cordillera Shear Zone. In addition, there is no significant correlation between ZHe ages and sample altitudes.

### Apatite (U–Th)/He ages

Apatite (U–Th)/He ages (AHe) are presented in Figure 1, and the analytical data are available in the Supplementary Material. Only a few of the ages contradict geological evidence. As with the ZHe results, no significant pattern was identified when comparing single-crystal He ages from a given sample with the corresponding eU or crystal size (e.g. Flowers *et al.* 2009; Murray *et al.* 2016).

In contrast to the zircon results, however, the apatite single-crystal aliquot ages are much more dispersed, and can be clustered into three groups (Fig. 1). The three oldest samples yielded Permian ages, followed by a triplet of Jurassic–Cretaceous ages and, finally, two mid-Cretaceous ages. Error bars overlap for samples within the same group, but do not extend from one group to another.

Another difference between the ZHe and AHe datasets is that the latter displays variability as a function of sample location. In general, samples collected in the hills of the northern section of the Uruguayan Shield, close to the border of the Norte Basin, yielded the oldest (Permian) cooling ages. In contrast, the youngest ages (i.e. Jurassic to Cretaceous) were obtained almost exclusively in samples collected in the southern portion of the study area. Nonetheless, correlation between the apparent AHe age and altitude is only moderate ( $r = 0.71$ ).

### Modelled thermal histories

Thermal modelling with HeFTy performed remarkably well for the obtained (U–Th)/He dataset with the assumed constraints. Usually data from three dated crystals were considered, but two of the models (sample UY-69-14 and the combination of samples UY-43-14 and UY-45-14) provided too few matching paths and had to be calculated on the basis of only two apatite and zircon crystals each. Such a positive output from models considering as many as six crystals at the same time is an indication of consistency in the dataset.

The same dataset was used in models with distinct configurations to test the validity of different hypotheses (summarized in Table 1) and for comparison of the trajectories that responded best to the measured parameters.

The exhumation events identified by the thermal models mostly reflect the periods within which the majority of (U–Th)/He ages are concentrated (Fig. 4). Based on the mean fits of all tested models, the ZHe temperature range is characterized by steep cooling trajectories mostly between 550 and 450 Ma. Cooling events constrained by the AHe dataset, in contrast, are divided into two distinct time intervals, the first from *c.* 160 to 120 Ma and the second from *c.* 100 to 80 Ma. Their presence in all models tested with different configurations indicates that these periods most probably correspond to actual cooling events. A third set of AHe results, corresponding to ages around the Permo-Triassic boundary, obtained a less conspicuous confirmation from the *T–t* modelling, having been identified only in some of the tested hypotheses.

All four of the tested hypotheses produced model temperature trajectories with at least acceptable fits to the measured data. As a

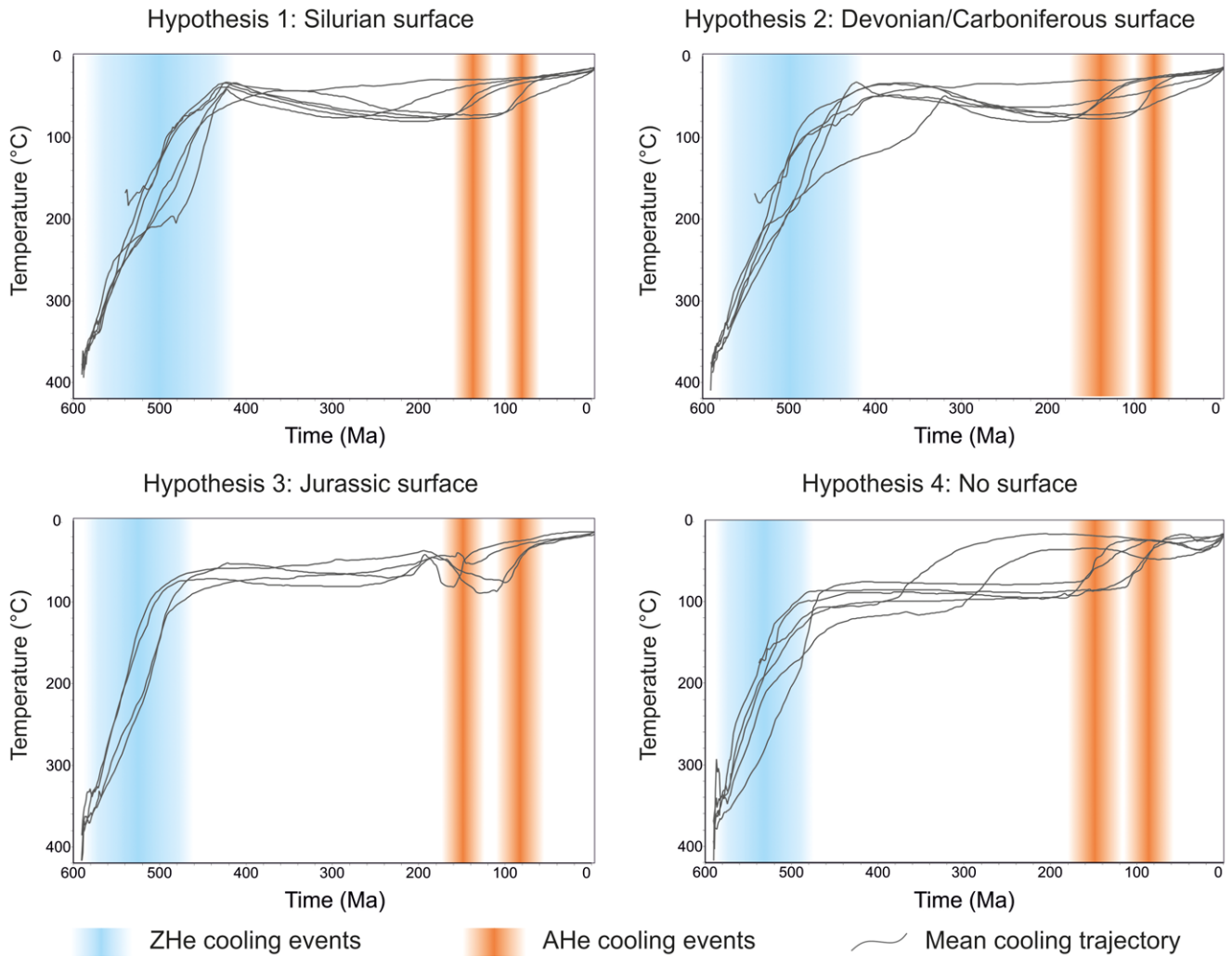


**Fig. 4.** Mean  $T-t$  trajectories of the modelling runs performed for the four hypotheses, with indication of the main exhumation events identified. Models were run 100 000 times or until obtaining the 100th good fit, and, with the exception of the constraints specific to each hypothesis, configurations were kept as similar as possible for comparison purposes.

result, none of the hypotheses can be ruled out as unrealistic geological trajectories. Some of the models, however, performed better than others. Their relative performance was initially tested on the basis of goodness of fit (GOF) values given by the software. A comparison of the GOF values among the best fits obtained for each model, however, proved to be of little diagnostic value for models with large numbers of path counts. Under all four hypotheses, increasing the numbers of model runs tended to raise GOF values until they stabilized around optimal values. Adding more model runs beyond this cutoff point failed to provide a gain in diagnostic model quality.

Given this limitation, a second criterion was used to compare the four hypotheses. For each model, the number of good trajectories was divided by the total number of tested paths. Direct comparison of these ratios was made possible by standardizing the constraints on the models under different configurations, thereby reducing the variability of parameters other than those specific to each hypothesis. This second criterion was found to exhibit much larger dispersion than the overall GOF values, and was thus deemed better suited to assessing the different scenarios.

A comparison of the overall values for all models shows that Hypotheses 1 and 2 consistently yielded the most elevated ratios (Fig. 5a). Hypothesis 3 clearly produced the lowest values, with results that are at least one order of magnitude below those for the remaining models. Finally, Hypothesis 4 maintained an

intermediate position. The consistent underperformance of Hypothesis 3 indicates that, although this hypothesis cannot be rejected, it is less likely to correspond to the actual geological evolution of the study area. The relationship between results from the remaining hypotheses is presented more clearly by comparing the results for each modelled sample (Fig. 5b). This representation clarifies that the results yielded by Hypothesis 2 are of a significantly lower quality than those of Hypotheses 1 and 2, with ratios varying from 2.5 to 30 times lower than those of the best-performing hypothesis. Although Hypotheses 1 and 2 produced comparable values for almost all modelled samples, it should be pointed out that even among them there is a consistent difference, with Hypothesis 1 producing the highest-performing ratios in all but one of the tested samples.

A few samples stand as exceptions to the overall pattern established above. UY-43-14 and UY-45-14, which were treated together, are the only samples for which Hypothesis 1 is not the highest performing scenario. Instead, Hypothesis 2 yielded a good/total-paths ratio that is *c.* 20% higher than in the case of Hypothesis 1. Although it forms an outlier in the dataset, this relative ratio for both hypotheses is completely within the range of most modelled samples. Sample UY-51-14, in contrast, is the only sample where Hypothesis 2 was the lowest-performing scenario among all tested configurations. In fact, its good/total paths ratio is about three times lower than that of the second-to-last low-performing model,



## Low-temperature evolution of the Uruguayan Shield

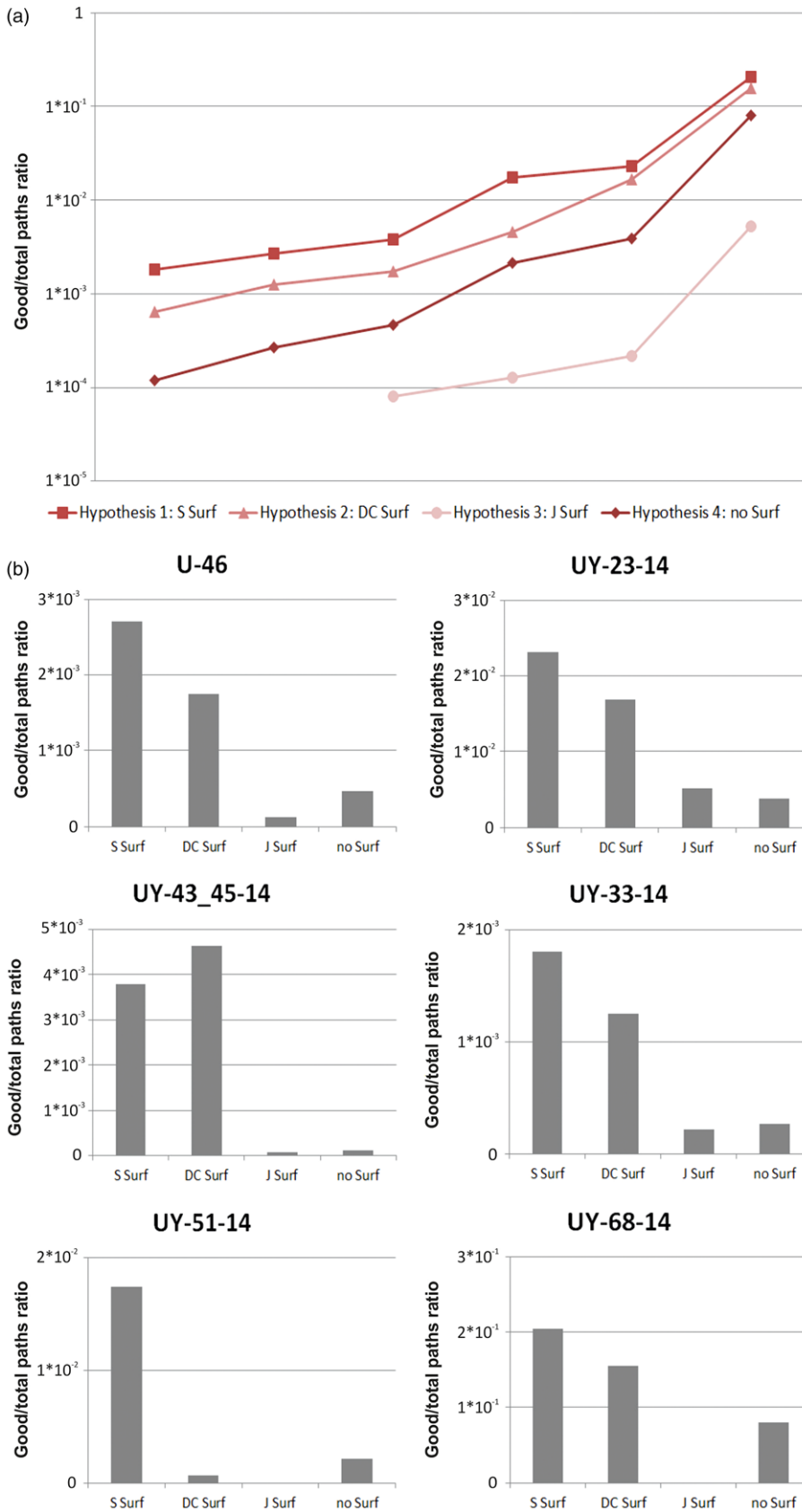


**Fig. 5.** Variation of the good fits/total tested paths ratios of the modelled dataset. (a) Comparison of ratios for all samples under the four tested hypotheses, arranged from the lowest-performing sample to the highest. It should be noted that the vertical scale is logarithmic. (b) Ratios from all tested hypotheses for each modelled sample. Vertical scale is linear. All models were run 100 000 times or until obtaining the 100th good fit. With the exception of the few constraints specific to each hypothesis, configurations were kept as similar as possible for comparison purposes.

Hypothesis 4, and almost 30 times smaller than the results from Hypothesis 1. Such an outlier strongly indicates that, unlike the other samples, a geological evolution compatible with Hypothesis 2 is unlikely for this sample.

In summary, the comparison of the ratio of good/total modelled paths seems to be a useful diagnostic parameter for the modelled

dataset, allowing for a direct comparison of different scenarios. Although the successful modelling of all tested configurations prevents a simple dismissal of any given hypothesis, the consistent relations between the obtained results strongly suggest that Hypothesis 1 most probably describes the geological evolution of the Uruguayan Shield, followed by Hypothesis 2, which also

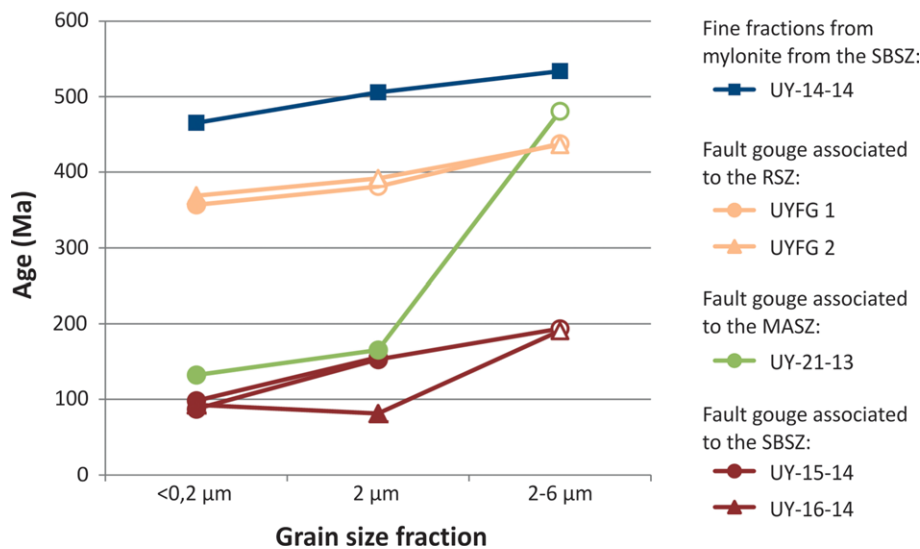


**Fig. 6.** K–Ar ages obtained on fine fractions and fault gouge of the Uruguayan Shield, arranged according to the dated grain-size fraction. Open symbols represent ages that could not be correlated to other geochronological methods or geological evidence. RSZ, Rivera Shear Zone; MASZ, Maria Albina Shear Zone; SBSZ, Sierra Ballena Shear Zone.

constitutes a realistic model. Hypothesis 4, and particularly Hypothesis 3, on the other hand, underperformed consistently. Accordingly, they can be interpreted as less likely descriptions of the thermal evolution of the (U–Th)/He dataset. Variations to the regional pattern recorded at restricted locations, however, suggest that the study area did not always act as a homogeneous entity.

### K–Ar results

K–Ar ages are presented in Figure 1. Double-sampled and double-measured gouge materials show excellent reproducibility, with results that mostly overlap within error. Both in the case of fine fractions and of fault gouge, K–Ar ages are grain-size dependent, increasing from finer to coarser fractions, a characteristic commonly referred to as inclined age spectra (Fig. 6).

As a maximum age to the faulting event recorded in the fault gouge samples from the Sierra Ballena Shear Zone, fine sericite fractions of the mylonites hosting the sampled rock were analysed (sample UY-14-14). The three grain-size aliquots produced K–Ar ages that range approximately from 535 to 465 Ma. Illite crystallinity analyses were performed on these samples to infer the metamorphic conditions under which they crystallized. Kübler Index values ranged between 0.139 and 0.185, pointing to temperatures above 300°C; that is, within the epizone (Kübler 1967).

Fault-gouge ages can roughly be divided into those from the Palaeozoic Era and those from the Mesozoic Era. Samples collected in the Isla Cristalina region, associated with the Rivera Shear Zone, yielded exclusively Palaeozoic ages, ranging from *c.* 440 to 360 Ma. These materials have very high K<sub>2</sub>O contents, with values as high as 8 wt%, indicating a mineral composition with abundant highly evolved K-rich illite, pointing to crystallizing conditions in excess of 250°C. Explicit analytical data on the clay mineralogy of this sample are not available.

Mesozoic ages were recorded on the fault gouge samples associated with the Sierra Ballena Shear Zone and the Maria Albina Shear Zone. These materials yielded results that mostly range from 195 to 80 Ma. They can roughly be divided into three groups. Two Early Jurassic ages (190–195 Ma) were obtained from the 2–6 μm fractions of both samples collected on the Sierra Ballena Shear Zone. They are followed by a set of results clustering around the Jurassic–Cretaceous boundary, ranging from 165 to 130 Ma, obtained from the <2 μm fraction of the fault gouge from the Sierra Ballena Shear Zone and from both the <2 and <0.2 μm fractions from the fault associated with the Maria Albina Shear Zone. Lastly, the <0.2 μm fractions of the gouge from the Sierra

Ballena Shear Zone yielded Late Cretaceous ages, ranging from 80 to 100 Ma. Standing out from these results, the <6 μm grain fraction of the gouge associated with the Maria Albina Shear Zone produced a K–Ar age of 481 ± 5 Ma.

Despite this consistent set of results, the set of samples that yielded Mesozoic ages shows a very low K<sub>2</sub>O content, close to the detection limit of the method. XRD mineral identification analyses indicate that most of the measured material consists of kaolinite, whereas illite is only an accessory mineral (*c.* 5 wt %). This low mineral concentration in both samples prevented the performance of analyses focused on determining the temperature conditions in which the analysed material was formed, such as illite crystallinity (Kübler Index) and polytypism.

It is possible to roughly estimate strain axes associated with the sampled faults during their activity based on preliminary kinematic data collected during the field investigation. These include the orientation of the fault surface, striae and the displacement of its passive markers or ‘R’ shears. This investigation was possible on the faults sampled along the Maria Albina Shear Zone and the Sierra Ballena Shear Zone, indicating a NE–SW principal stress orientation and a transtensional strain during the Cenozoic faulting events.

### Discussion

#### Comparison of modelled thermal histories

The thermal modelling of the analysed samples produced successful results for all tested hypotheses (outlined in Table 1), suggesting that none of the configurations can be rejected as unrealistic descriptions of the thermal history of the Uruguayan Shield. However, a comparison of the performance of each hypothesis has shown that some of the configurations have consistently produced better results than others.

The best-fitting thermal paths were obtained by the constraints imposed in Hypotheses 1 and 2. Both scenarios consistently yielded more paths that could be classified as good fits with the modelled dataset and clearly outperformed the competing models in almost all tested samples. They share some of their assumptions, proposing early post-orogenic exhumation and exposure to surface conditions during the early and middle Palaeozoic. As such, it is strongly suggested that initial exhumation after the Brasiliano Orogeny during the early Palaeozoic was responsible for exposing the analysed samples to near-surface conditions. This agrees well with previous geochronological data in the region, which indicate late-stage low-degree deformation immediately before the onset of the cooling event defined by the ZHe ages (Oyhantçabal *et al.* 2011b;

Oriolo *et al.* 2015, 2016b,c), as well as with the K–Ar dating of fine fractions presented in this work. In addition, provenance studies of the earliest sediments of the Norte Basin in Uruguay suggest that most Precambrian terranes in Uruguay acted as source areas during the Devonian (Uriz *et al.* 2016), which implies that the studied rocks should have been exposed to the surface by then.

Another implication of the high performance of Hypotheses 1 and 2 is that initial exposure of the Uruguayan Shield to surface conditions was followed by reheating during the Palaeozoic, resetting the AHe system. This heating event was probably caused by deposition of the sedimentary sequences of the Norte Basin, and affected rocks currently cropping out in the landscape. It is therefore likely that the Paraná Basin previously extended beyond its current boundaries, with some of its sedimentary strata covering portions of the crystalline basement that are now exposed. This agrees well with evidence that a considerable portion of the sedimentary packages was eroded from the margins of the basin (e.g. de Santa Ana 2004; Milani *et al.* 2007; Strugale *et al.* 2007). This is also in accordance with other recent thermal modelling data from basement areas in Uruguay and southern Brazil (Kollenz 2015; Oliveira *et al.* 2015). This cycle of deposition and erosion probably preceded the onset of flood-basalt eruption, and may have been controlled by the onset of NW–SE-trending deformation of the basin (e.g. Rostirolla *et al.* 2000; Strugale *et al.* 2007).

The relatively poor performance of Hypothesis 3, which assumed exposure to surface conditions during the Jurassic Period, suggests that the thick Cretaceous volcanism did not have a decisive impact on the thermal evolution of the analysed samples. In this sense, the coeval ages obtained with both the (U–Th)/He and K–Ar methods probably record the occurrence of tectonic displacement and exhumation accompanying the rifting of the South Atlantic Ocean and of the Santa Lucia–Aiguá–Merín Lineament corridor, rather than the resetting of the geochronological system by the thermal effect of Paraná flood basalts. As such, the extrusive event was probably confined to its present occurrence, as exemplified in the Santa Lucia–Aiguá–Merín Lineament corridor, where the disposition of the volcanic rocks has been restricted to the basins hosted by the rift corridor. Whereas these areas experienced subsidence from the Cretaceous Period onwards, their surroundings have since been exhumed (Rossello *et al.* 2007).

Somewhat more surprising is the poor performance of Hypothesis 4 among the tested models. As such, it argues against a straightforward assumption that the Uruguayan Shield went through a simple exhumation trajectory, without the effect of previous exposure of the current terrain to surface conditions or to a reheating event.

Some of the models yielded results that differ from the general pattern established by most samples. The clearest example is sample UY-1-15, which experienced a final exhumation during the transition from the Carboniferous to the Permian. This implies a vertical displacement considerably larger than in the rest of the study area. This is indicative that the Uruguayan Shield did not behave uniformly, having on occasions involved strong contrasts in the magnitudes of crustal displacements in contiguous areas. The timing of final exhumation to current crustal depths is variable across the study area, as indicated by the variability in apparent AHe ages.

### K–Ar ages

Samples dated by the K–Ar method are grain-size dependent; that is, they produce inclined age spectra (Fig. 6). This pattern is commonly identified in the literature for pelitic rocks, and is usually interpreted as mixing of detrital muscovite with the neoformation of sericitic crystals. Nonetheless, a similar pattern has also been recognized in fault gouge (e.g. van der Pluijm *et al.* 2001; Clauer

*et al.* 2012; Bense *et al.* 2014; Torgersen *et al.* 2015; Ksienzyk *et al.* 2016). The most credited interpretation for this behaviour is also related to a mixing of different age components, either because of the crushing of host-rock minerals or because of an inheritance of illite from older generations of fault reactivation. It is generally assumed that the finest fractions of the fault gouge are less affected by the contamination of host rocks (Torgersen *et al.* 2015; Ksienzyk *et al.* 2016), making their ages the most reliable when dating brittle faulting events.

The inclined age spectrum obtained for the fine fractions of the mylonitic wall-rock to the fault associated with the Sierra Ballena Shear Zone might be interpreted as similar in origin to that of pelitic rocks. In this case, the 2–6  $\mu\text{m}$  fraction might represent inherited muscovite crystals crystallized during the ductile stage of the shear zone. As such, assuming that this grain fraction is the most susceptible to contamination, its age of  $534 \pm 8$  Ma can be admitted as an age limit for the end of mylonitization on this shear zone. This age happens to be less than 20 myr younger than the last U–Pb zircon age for a porphyritic mylonite along this structure (Oyhantçabal *et al.* 2011b). The generation of the finer and younger sericites at  $506 \pm 11$  and  $465 \pm 7$  Ma should represent stages of tectonic displacement along the shear zone following the mylonitic phase of the structure within the ductile–brittle transition. Nonetheless, the crystallization conditions above  $300^\circ\text{C}$  indicated by its degree of illite crystallinity (Kübler Index 0.139–0.185) are distinctly warmer than those indicated by the coeval ZHe data for the undeformed shield. They might, therefore, be related to the upward percolation of hydrothermal fluids along the fault zone during reactivation, as argued by Tagami (2012).

The Palaeozoic fault gouge associated with the Rivera Shear Zone produced ages that range from 360 to 440 Ma. The  $<0.2$   $\mu\text{m}$  fraction yielded ages that are close to the Devonian–Carboniferous boundary, which is recognized in most basins in SW Gondwana as a regional angular unconformity (López-Gamundi & Rossello 1993). In the Paraná Basin, specifically, it marks the top of the Paraná Supersequence, which is followed by a sedimentation gap that spans most of the Carboniferous Period (Milani *et al.* 2007). Coarser fractions from the same gouge provide ages that have a less clear interpretation, and might have been affected by some degree of contamination from the host rock.

The Mesozoic set of K–Ar results was recorded on both the Maria Albina Shear Zone and the Sierra Ballena Shear Zone, and is distinctively dependent on the grain size of the dated fraction. Three groups of ages were recognized: Early Jurassic, Jurassic–Cretaceous and Late Cretaceous. The last two sets, corresponding to results obtained in the  $<0.2$  and  $<2$   $\mu\text{m}$  fractions of gouge samples associated with both shear zones, have ages that correspond well to time periods recorded by the AHe dataset. They correlate well with the pre-, syn- and post-rift phases of the South Atlantic Ocean. The 2–6  $\mu\text{m}$  fractions from both faults produced results that, in contrast, have a less clear geological interpretation. The material dated from the gouge related to the Maria Albina Shear Zone stands out for having a very old age of *c.* 480 Ma. This age is well within the range of fine fractions dated for the wall-rock of another structure, the Sierra Ballena Shear Zone, and is probably the result of contamination from sericite crystals from the host rock. As such, it should not be interpreted as representative of a brittle event in this shear zone. Similarly, the pair of ages of *c.* 190–195 Ma from the 2–6  $\mu\text{m}$  fraction of the gouge associated with the Sierra Ballena Shear Zone cannot be correlated to other low-temperature data and have no clear relation to known geological events. As this fraction is the most susceptible to contamination from minerals from the host rock, these ages are not considered in this study to be representative of faulting events.

In summary, the new K–Ar ages obtained can be correlated with other low-temperature geochronological methods and regional

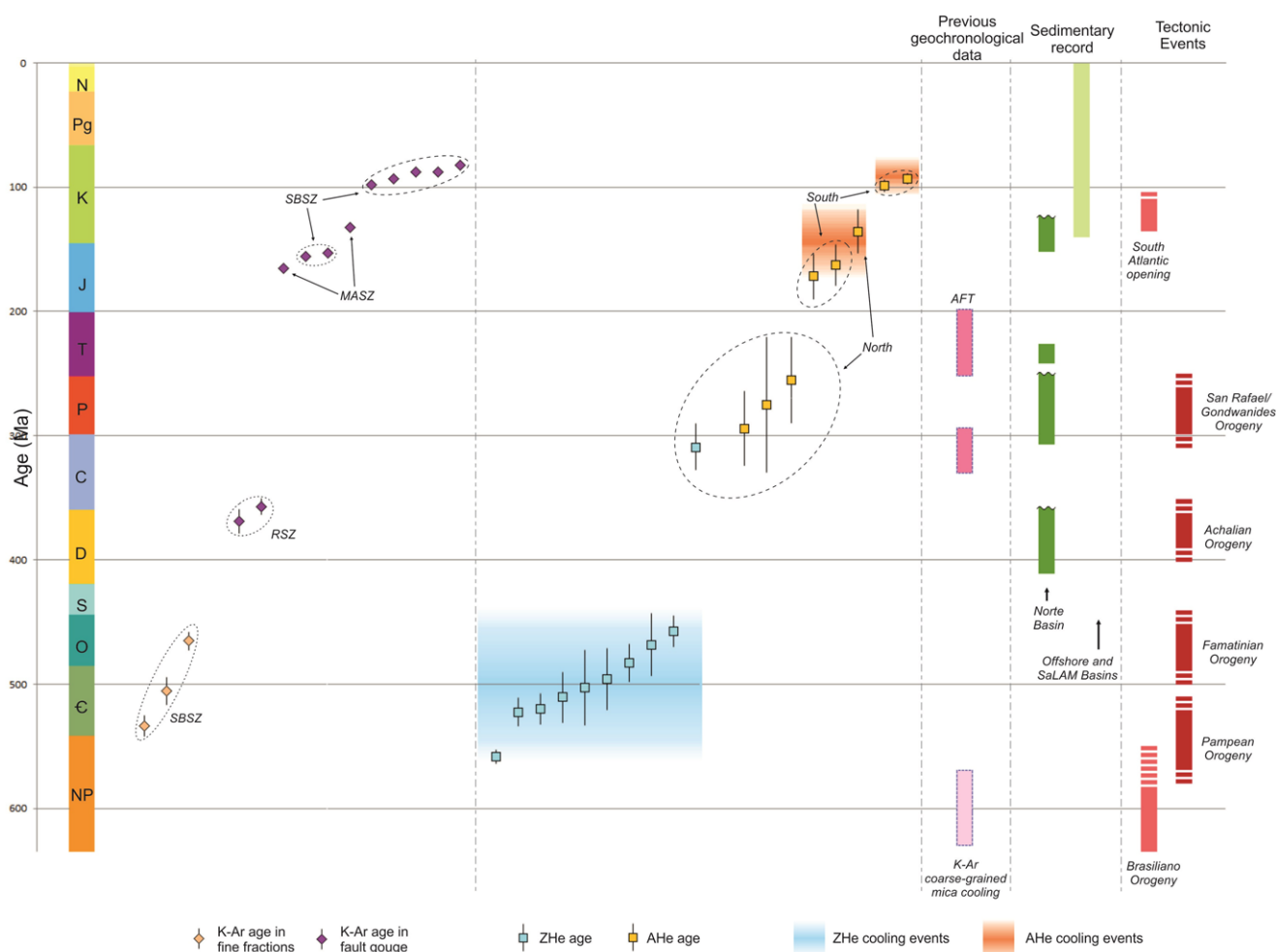


**Fig. 7.** Temporal distribution of low-temperature geochronological data in relation to main sedimentary and tectonic events. Error bars represent  $2\sigma$  imprecision. Time constraints for the AFT method are from [Kollenz \(2015\)](#) and K–Ar cooling ages of coarse-grained mica are from [Oyhantçabal \*et al.\* \(2009b, 2011a\)](#) and [Oriolo \*et al.\* \(2016a,b\)](#). RSZ, Rivera Shear Zone; MASZ, Maria Albina Shear Zone; SBSZ, Sierra Ballena Shear Zone.

geological events. The inclined age spectra obtained in the fault gouge samples probably result either from contamination of the host rock (in the case of outlying ages) or from recurrent reactivation of the geological structures, in the latter case generating more than one geologically meaningful age in the same sample.

### Low-temperature evolution of the Uruguayan Shield

By combining different low-temperature geochronological methods, the new dataset reveals more than 450 myr of late- to post-orogenic tectonic evolution since the beginning of the Palaeozoic Era. [Figure 7](#) presents a graphic summary of the new ages and illustrates their temporal relation to the Uruguayan sedimentary record and the regional tectonic events in western Gondwana, alongside previous medium- and low-temperature geochronological data.

Formerly published apatite fission track (AFT) ages ([Kollenz 2015](#)) mostly cluster between 245 and 200 Ma, but there are also considerable older apparent ages of *c.* 300 and 325 Ma. The AFT ages are usually between the ZHe and AHe ages, attesting to the consistency of the database in the region.

The widespread distribution of ZHe ages between 560 and 460 Ma within a large-scale area differs from previous studies in southern and SE Brazil for similar temperature ranges (ZFT and ZHe ages). Such old signatures, if present at all, are usually limited to a few samples within generally younger domains (e.g. [Karl \*et al.\* 2013](#)). This is probably a reflection of the significant uplift

experienced in these areas during the post-rift opening phases of the South Atlantic Ocean, as evidenced by its coastal ranges and numerous thermochronology studies (e.g. [Tello Saenz \*et al.\* 2003](#); [Hackspacher \*et al.\* 2004](#); [Franco-Magalhães \*et al.\* 2010, 2014](#); [Cogné \*et al.\* 2011, 2012](#)). This new pattern points to the relevance of applying such techniques to regions of lower relief such as Uruguay, leading to a more detailed Phanerozoic history (e.g. [Oliveira \*et al.\* 2015](#)).

The continuous distribution of Palaeozoic ZHe ages between 560 and 460 Ma suggests that they are not related to single events but rather to a period during which the sampled crystals crossed the partial retention zone. As such, the Uruguayan Shield probably behaved as a consolidated unit already during the beginning of the Palaeozoic and underwent significant exhumation since the Ediacaran, driving the analysed samples to relatively shallow depths. This is corroborated by the thermal modelling of the (U–Th)/He dataset, which shows steep cooling trajectories for this period. Further indication of early Palaeozoic tectonic activity is given by the K–Ar ages for the fine sericite fractions of the Sierra Ballena Shear Zone mylonite.

This event extends into the border of the Piedra Alta Terrane, with sample UY-68-14 recording the first Palaeozoic cooling ages in this geological unit. Because muscovite K–Ar cooling ages are restricted to the Palaeoproterozoic Era within this unit ([Oyhantçabal \*et al.\* 2011a](#)), these rocks are expected to have been exposed to surface conditions much sooner than the recorded ZHe ages. Therefore, the new results indicate a Brasiliiano-aged gentle

thermal overprint of the border of the Rio de la Plata Craton, which did not, however, reach temperatures high enough to affect the muscovite K–Ar system. Such burial conditions match the shallow emplacement interpreted for the only Neoproterozoic intrusion in the Piedra Alta Terrane, the La Paz Granite ( $587 \pm 8$  Ma, [Cingolani et al. 2012](#)). Further into the centre of the Rio de la Plata Craton, sample UY-1-15 yielded an apparent ZHe age of  $309 \pm 19$  Ma, which is almost 140 myr younger than the remaining ZHe results, breaking away from the pattern of continuous post-collisional ages established above.

In terms of the thermal range and, as a consequence, crustal depth, the new geochronological dataset shows a distinctive contrast between the Dom Feliciano Belt in Uruguay and the orogenic belts on the African side of the Atlantic. The new ZHe data are coeval with regional K–Ar and Ar–Ar muscovite-cooling ages for the Kaoko, Damara, Gariep and Saldania belts, which have consistently been dated as younger than 530 Ma ([Goscombe et al. 2005](#); [Gray et al. 2006](#); [Foster et al. 2009](#), and references therein). They were interpreted to represent the last phases of the Pan-African Orogeny on the African continent, particularly the late stages of interaction between the Congo and Kalahari Cratons.

This relation suggests a common tectonic drive, causing concurrent exhumation processes in adjacent areas of the Gondwana supercontinent during its last phases of assembly, but at distinct crustal depths. It can be interpreted as an immediate effect of the final phases of the Brasiliano Orogeny itself, with tectonic exhumation associated with post-collisional extension of the thick continental crust (e.g. [Constenius 1996](#); [Çemen et al. 2006](#); [Fossen 2010](#)). This is corroborated by the fact that the new set of ages is only a few tens of million years younger than the late stages of deformation and magmatism in the Dom Feliciano Belt and Nico Pérez Terrane ([Hartmann et al. 2002](#); [Basei et al. 2005, 2013](#); [Campal & Schipilov 2005](#); [Oyhantçabal et al. 2011b](#); [Oriolo et al. 2016a](#)). Furthermore, effects of extensional tectonics have been inferred to begin along the Dom Feliciano Belt as early as 600 Ma ([Almeida et al. 2010, 2012](#)).

Another possible influence on the early Palaeozoic thermal history of the Uruguayan Shield is the continuous orogenic history along the active SW Gondwana margin. The late phases of the Pampean and early Famatinian events ([Steenken et al. 2011](#), and references therein), in particular, are coeval with the bulk of ZHe and fine fraction K–Ar data. This coincidence, however, is unlikely to entirely explain the data from this study because it does not account for the lack of low-temperature ages corresponding to the later events of this orogenic association.

The bulk of the ZHe dataset is followed by *c.* 140 myr during which no (U–Th)/He cooling ages were recorded. Rather than uplift, this period is better characterized by subsidence and reheating, as recorded by the onset of Paraná Basin deposition. The thermal modelling performed with the new (U–Th)/He dataset corroborates this suggestion, indicating a reheating responsible for resetting the AHe system. At least during the Early Palaeozoic, parts of the basement might have been exposed and acted as a source area for these sediments, in agreement with provenance studies ([Uriz et al. 2016](#)). Tectonic activity was recorded only locally at the end of the Devonian, based on the K–Ar ages of two fault-gouge samples associated with the Rivera Shear Zone in the Isla Cristalina Block and with regional angular unconformities and a gap in the sedimentary record ([López-Gamundi & Rossello 1993](#); [Milani et al. 2007](#)).

The late Palaeozoic and Mesozoic eras in the Uruguayan Shield are recorded predominantly by the AHe data. Unlike the ZHe data, AHe results are much more varied and location-dependent. There is a striking difference between the northernmost and southernmost ages, which are separated by as much as 200 myr.

Considered together, the three oldest AHe ages and the youngest ZHe age define an interval from the end of the Carboniferous and

throughout the Permian (*c.* 310–250 Ma). They are much older than the subsequent AHe results, and are clearly associated with the northern part of the Uruguayan Shield; that is, along the present border of the Norte Basin. The two oldest AFT ages recorded in Uruguay ([Kollenz 2015](#)), also obtained from the northern part of the shield, are approximately contemporaneous.

Among these results, sample UY-1-15 is an outlier. Besides having a much younger ZHe age, it is the only sample for which both the ZHe and the AHe ages are almost identical, overlapping at the transition from the Carboniferous to the Permian. Unlike the other samples, this implies a faster and steadier exhumation to present conditions, without multiple events or burial periods. Consequently, there should be a fault separating the inner portion of the Piedra Alta Terrane from its boundary, at least in the north. We hypothesize that the coeval exhumation of rock units under contrasting temperature conditions was accommodated by this fault.

It should be noted, however, that this time interval was not constrained by the *T–t* models as precisely as the later events (Mesozoic AHe ages). Likewise, the Permo-Triassic set of ages is not always represented by cooling trajectories in the thermal models. This suggests that the ages do not necessarily correspond to sharp exhumation events, and might be related instead to only partial resetting of the AHe isotopic system. This is also suggested by the fact that this period corresponds to the deposition of the thickest Palaeozoic sedimentary package in this basin (Gondwana I Supersequence, [Milani et al. 2007](#)).

There seems to be, however, a correlation between these localized ages and the presence of angular unconformities in this sedimentary package ([Milani et al. 2007](#); [Rocha Campos et al. 2006](#)). These have been interpreted as resulting from far-field propagation of compressional deformation into the continent ([Rostirolla et al. 2000](#); [de Santa Ana 2004](#); [Pángaro et al. 2015](#)), linked to the development of the Gondwanides–San Rafael Orogeny along the active margin of the supercontinent ([von Gosen et al. 1990](#); [Kleiman & Japas 2009](#); [Sato et al. 2015](#)). Similar effects have been reported, for example, from the Sierras Pampeanas in Argentina ([Löbens et al. 2011](#); [Bense et al. 2014](#)).

All factors considered, the set of oldest AHe ages is not necessarily linked to exhumation of the Uruguayan Shield, but the presence of local cooling events cannot be ignored. These would indicate that, despite covering a large intracratonic area, subsidence in Uruguay was not spatially uniform and may have coexisted with local exhumation, especially in the north.

The transition to the Triassic Period is recorded in Uruguay by the bulk of the AFT results of [Kollenz \(2015\)](#), indicating a more regional exhumation. It correlates with the extensional tectonics that characterizes this period in South America, recorded in the Paraná Basin by the development of restricted grabens ([Zerfass et al. 2004](#)).

The remaining ages, including the Mesozoic set of K–Ar results in fault gouge samples, are mostly restricted to the southern portions of the Uruguayan Shield. They range from the Late Jurassic to the Cretaceous and are linked to the opening of the South Atlantic Ocean. Three main episodes can be distinguished: a Late Jurassic, an early Cretaceous and a mid-Cretaceous event, corresponding to the doming, syn- and post-rift phases, respectively. The first is recorded by a couple of AHe and K–Ar ages (<2  $\mu$ m sericitic fractions from fault gouge) associated with the Maria Albina Shear Zone and the Sierra Ballena Shear Zone. These ages range from 175 to 150 Ma, and represent early exhumation in response to the thermal anomaly that led to continental rifting.

The phase of rifting itself, coeval with the extensive basaltic magmatism in the Norte and Laguna Merin basins, is recorded by one AHe age and by the K–Ar dating of a fault gouge related to the Maria Albina Shear Zone. Of the new results, the AHe age stands out for being the only one north of the Santa Lucia–Aiguá–Merin

Lineament corridor younger than Palaeozoic, and may be related to a slight exhumation of the corridor's northern border, as recognized by Rossello *et al.* (2007). These ages are contemporaneous with the c. 135–130 Ma Paraná volcanism (Renne *et al.* 1992; Janasi *et al.* 2011; Cernuschi *et al.* 2015). Thermal modelling suggests that this extrusive event had little effect on rocks from the crystalline basement, and that the flood basalts were probably confined to the areas where they presently occur.

A younger and larger set of data, ranging from 100 to 85 Ma, is represented by two AHe ages and by the K–Ar ages of the <0.2  $\mu\text{m}$  fractions of fault gouge samples associated with the Sierra Ballena Shear Zone. These data correlate well with the beginning of the main exhumation process that culminated in the uplift of the coastal ranges in south and SE Brazil (Franco-Magalhães *et al.* 2010; Cogné *et al.* 2011, 2012; Karl *et al.* 2013, and references therein). In contrast to these results obtained in the latter areas, however, there is a notable absence of Cenozoic AHe data in Uruguay. This can be explained by the low denudation rates mirrored by the gentle topography of the region.

Thermal modelling of the (U–Th)/He dataset identified two main stages of cooling during the Mesozoic, strengthening the interpretation that the combined AHe and K–Ar ages correspond to actual exhumation events. The first phase broadly corresponds to the pre- and syn-rift ages, whereas the second is associated with the post-rift event. In this regard, these events are compatible with the two palaeosurfaces identified by Panario *et al.* (2014), which those researchers interpreted to have a Mesozoic origin.

### ***Influence and reactivation of Brasiliano structures during the Phanerozoic***

One of the main characteristics of orogenic events is the assembly of a complex structural configuration, combining fault zones at all crustal levels with variable rock fabrics. The result is a highly anisotropic crust, in which the influence of weaknesses along preferential orientations has a significant control on subsequent deformation. As such, an inherited structural framework has a lasting influence on the tectonic evolution of the newly formed terrane long after the cessation of the orogeny itself, an aspect that has received much scientific interest in recent decades.

The effect of the reactivation of old discontinuities on rifting processes cannot be understated. It is a prominent mechanism in the formation of basins of all sizes and in all geotectonic contexts, with the potential for influencing the basins' location, shape and evolution (e.g. Milani & Davison 1988; Morley *et al.* 2004; Riccomini *et al.* 2004; Autin *et al.* 2013; Peron-Pinvidic *et al.* 2013; Figueiredo *et al.* 2015). Thermochronological techniques have recently started to be widely applied to such contexts, not only to date the faulting events but also to identify relative displacements (e.g. Franco-Magalhães *et al.* 2010; Ksienzyk *et al.* 2016; Tremblay *et al.* 2013; Fossen *et al.* 2016).

One of the major aspects that control the influence of previously formed structures during rifting is the angle formed between the older fabric and the direction of the subsequent regional extension in the area. As has been shown both in natural examples and in models, pre-existing faults with angles as high as 45–60° to the orientation of the extension vectors tend to be reactivated with oblique displacements, accommodating extension along old weaknesses instead of creating new discontinuities (Morley 1995; Morley *et al.* 2004; Henza *et al.* 2011). Even along structures with less favourable orientations (i.e. orientations that are not decisive during strain concentration), minor reactivation can still influence rift evolution by creating domain boundaries (Fossen *et al.* 2016).

The recurrent reactivation of Brasiliano-related shear zones during the Phanerozoic evolution of the Uruguayan Crystalline Shield is distinctively evidenced by the dating of multiple brittle

events on fault gouge materials generated along them. These ages correlate chronologically with the rest of the low-temperature dataset and can be linked to regional events that probably influenced its evolution. Kinematic analysis of structural data associated with faults that yielded early and mid-Cretaceous K–Ar ages indicate transtensional strain with principal stress oriented NE–SW. This observation is in accordance with the orientation of syn- and post-rift stress fields at the time in south and SE Brazil (Salomon *et al.* 2015, and references therein).

Nevertheless, how exactly the Neoproterozoic shear zones influenced the exhumation history in Uruguay is not clear from the (U–Th)/He record. Because they do not divide blocks with consistently distinct ages in either of the analysed minerals, we infer that the vertical displacements of these events might not have been sufficient to be detected by these methods. The main geographical pattern observed in the new low-temperature dataset is the north–south difference observed among the AHe results. This finding is no surprise given the presence of ENE–WSW- and WNW–ESE-striking structures that were very active in the southern and SE portion of the South American shield since the early stages of Atlantic opening. Effects of this tectonic control include the deformation of intracratonic basins, segmentation of the passive margin and conditioning of the emplacement of basic dykes (Zalán *et al.* 1990; Rostirolla *et al.* 2000; Meisling *et al.* 2001; Strugale *et al.* 2007; Masquelin *et al.* 2009; Franco-Magalhães *et al.* 2010; Salomon *et al.* 2015). Their influence on late stages of exhumation has been shown to go back to more than 200 Ma in southern Brazil (Karl *et al.* 2013). It has also been shown to be a more dominant system in the southern portion of the Atlantic margin than further north, which is more affected by the reactivation of NE–SW-trending Brasiliano structures (Riccomini *et al.* 2004; Cogné *et al.* 2011, 2012, 2013; Franco-Magalhães *et al.* 2014).

In Uruguay, the most remarkable expression of this phase of deformation is the installation of the Santa Lucia–Aiguá–Merín Lineament, controlling an aborted rift during the Jurassic–Cretaceous transition. This corridor has been affected by the reactivation of structures in the basement inherited from the Brasiliano deformation. The orientation of the lineament is favoured by the foliation directions and subordinate shear zones within the eastern Dom Feliciano Belt (NE–SW; Oyhantçabal *et al.* 2009a; Oriolo *et al.* 2016b) and the Piedra Alta Terrane (east–west; Oriolo *et al.* 2015), which have been interpreted as influential aspects of the rift's development (Rossello *et al.* 2007).

This corridor is further influenced by the Sierra Ballena Shear Zone and Sarandí del Yí Shear Zone, the major terrane boundaries of the Uruguayan Shield, which act as internal limits to the basins deposited along the corridor. Although their orientation, which is parallel to the main extension vectors during rifting of the basement, means that they probably did not accommodate much of the extension, they separate an elevated internal domain, corresponding to the Nico Pérez Terrane, on which only disconnected Cretaceous metasedimentary remnants occur. The progress of the rifting process within this terrane was probably hindered by a less favourable, inherited structural framework (NNE–WSW; Oriolo *et al.* 2016b) preventing a connection of the Laguna Merín and Santa Lucia basins (Rossello *et al.* 2007). The multiple exhumation events identified in this study emphasize the importance of these structures during the synsedimentary evolution of the basins, acting as domain boundaries (e.g. Fossen *et al.* 2016) and possibly leading to some uplift, which would explain the relative elevation of the Nico Pérez Terrane.

### **Conclusions**

The application of low-temperature geochronological methods across the crystalline shield of Uruguay reveals an eventful

## Low-temperature evolution of the Uruguayan Shield

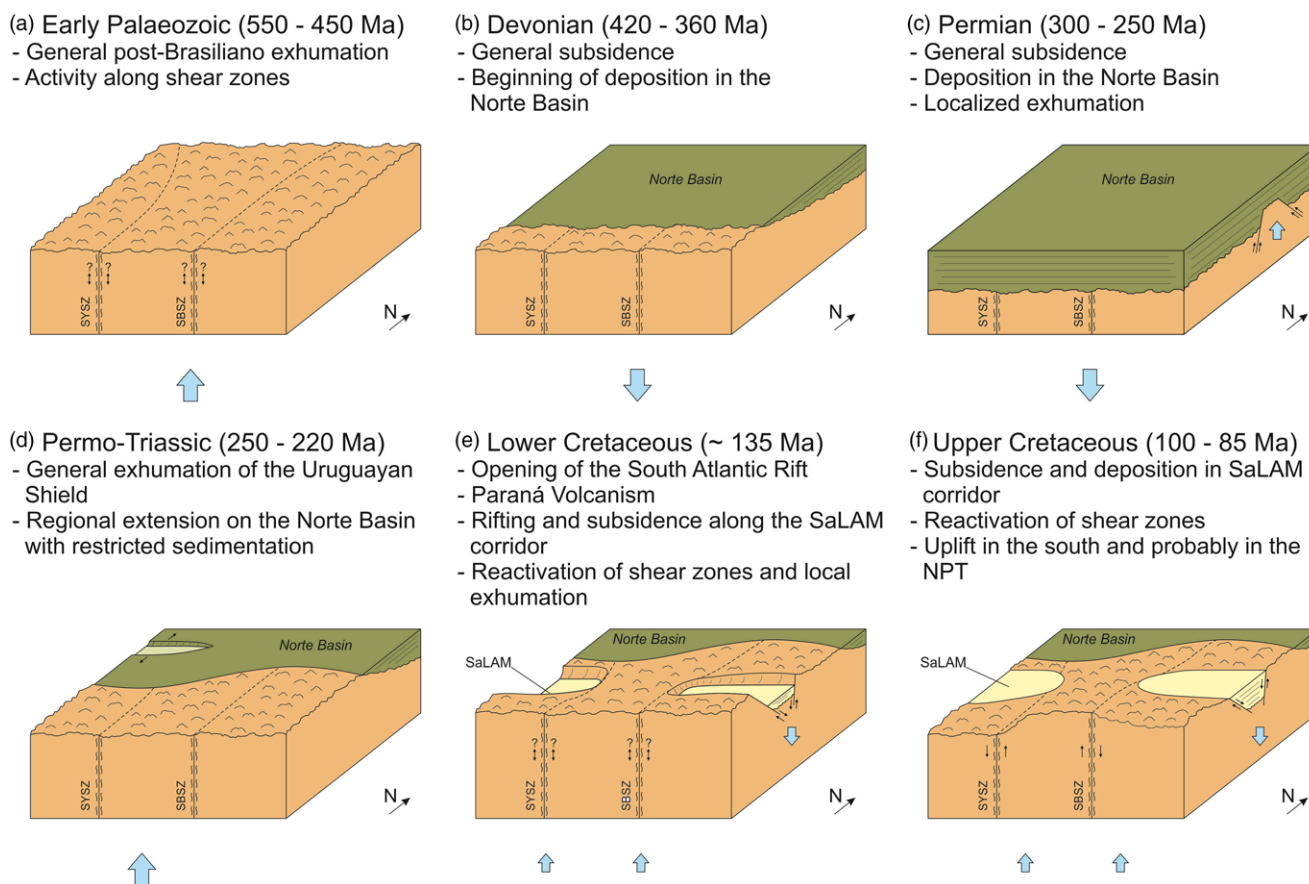


**Fig. 8.** Schematic evolutionary model of the Uruguayan Shield and associated sedimentary record during the Phanerozoic Eon. SYSZ, Sarandí del Yí Shear Zone; SBSZ, Sierra Ballena Shear Zone; SaLAM, Santa Lucia-Aiguá-Merín Lineament; NPT, Nico Pérez Terrane.

geological history throughout the Phanerozoic, revealing up to 550 myr of residence time in the upper crust. This study identifies with rare detail the discrete tectonic activity that has affected the interior of Gondwana and is connected with various independent clues in the sedimentary record. The reconstructed geological history is the result of low-intensity events compared with the uplift that characterizes the thermal record of much of the South American eastern passive margin. This study thus shows the advantages of applying thermochronological research to areas with less dramatic topography than along the Brazilian passive margin, where Cenozoic events have overprinted much of the low-intensity and much older signal recorded by our data.

As shown by the new data, all of the crustal blocks that compose the Uruguayan Shield reached shallow burial conditions between 550 and 450 Ma. Therefore, the terrane amalgamation was completed during the Ediacaran Period. The post-collisional period was marked by intense exhumation and tectonic activity, and thermal modelling strongly suggests that rocks currently cropping out were exposed to near-surface conditions by early to mid-Palaeozoic times (Fig. 8a). Multiple subsidence cycles promoted the Paraná Basin sedimentation, which began in the Devonian, during which the crystalline basement acted as a source area (Fig. 8b). The middle and late Palaeozoic were characterized by the further burial of the basement and resetting of the (U–Th)/He system until Permian time, when the thickest sedimentary package of the basin was deposited. The record of local exhumation indicates, however, that subsidence was not uniform in Uruguay (Fig. 8c).

During the Mesozoic, the basement rocks of Uruguay went through multiple cycles of exhumation, accompanied by restricted sedimentation. The Triassic was marked by general exhumation of the crystalline shield, and sedimentation was confined to portions of

the Norte Basin (Fig. 8d). After this event, the basement areas closest to the border of this basin were essentially in their present conditions. The southern portion of the study area went through additional phases of exhumation associated with the opening of the South Atlantic Ocean, accompanied by the installation of an aborted rift along the Santa Lucia–Aiguá–Merín Lineament corridor in the early Cretaceous (Fig. 8e). This event was recorded by the exhumation of rocks close to the corridor’s margin and by the reactivation of the main Neoproterozoic shear zones, dated by the K–Ar method in fault gouge samples. The last event detected in Uruguay is a post-rift phase of upheaval registered in the Early to Late Cretaceous transition. It is probably responsible for the uplift of the Nico Pérez Terrane and southeastern Dom Feliciano Belt, accompanied by more fault reactivation (Fig. 8f). In contrast to most areas along the SE Brazilian coast, a shorter post-rift geological evolution in Uruguay implied little exhumation during the Cenozoic.

The tectonic forces driving this evolution varied through time. Initial exhumation was coeval with the final stages of the Pan-African Orogeny, and followed late deformation of the Dom Feliciano Belt in Uruguay. From the Devonian to the early Mesozoic, the thermochronological record is less well constrained, and was probably controlled by the far-reaching tectonic influence of the southwestern active margin of Gondwana, leading to the development of the Paraná Basin. The last regional tectonic drive was the opening of the South Atlantic Ocean and its associated rifts, which dominated the final exhumation and uplift of the Uruguayan Shield.

Thermal modelling of the new dataset suggests that the Paraná Basin once covered much of the now-exposed crystalline basement, which had already been exposed to near-surface conditions prior to burial by the Paraná sequences. This resulted in resetting of the

basement AHe system, with the reheating most probably accomplished by the deposition of the Palaeozoic sedimentary sequences, in particular by the Devonian and Permian sediments. The thick flood basalts, still present in the Norte and Laguna Merin basins, had little influence on the studied rock's thermal histories. Unlike the older Palaeozoic sedimentary rocks, the palaeogeography of the basalts was probably confined to their present occurrence.

Inherited Neoproterozoic structures played an important role in the post-Brasiliano history. Although the major shear zones do not define the boundaries observed in the (U–Th)/He age pattern, the last phases of exhumation are clearly coeval with K–Ar-dated fault reactivation. The rifting and subsidence pattern of the Santa Lucia–Aiguá–Merin Lineament corridor were strongly conditioned by the legacies of crustal anisotropy, and likewise were segmented by the main Brasiliano shear zones despite the fact that these probably did not accommodate much of the extension. This activity is possibly related to differential exhumation during the final stage of uplift, which has shaped the modern landscape of Uruguay.

**Acknowledgements** The authors are grateful for helpful comments and suggestions from three reviewers and for the careful input of editor Y. Gunnell.

**Funding** M.H. would like to thank the CNPq for a long-term PhD scholarship from the Sciences without Borders programme. S.O. thanks DAAD for a long-term PhD scholarship (A/12/75051).

*Scientific editing by Yanni Gunnell*

## References

- Almeida, F.F.M., Amaral, G., Cordani, U.G. & Kawashita, K. 1973. The Precambrian evolution of the South American cratonic margin, South of Amazonas River. In: Nairn, A.C.M., Kanes, W.H. & Stehli, F.G. (eds) *The Ocean Basins and Margins*. Plenum, New York, 411–446.
- Almeida, F.F.M., Hasui, Y., de Brito Neves, B.B. & Fuck, R.A. 1981. Brazilian structural provinces; an introduction. *Earth-Science Reviews*, **17**, 1–29.
- Almeida, R.P., Janikian, L., Frago-Cesar, A.R. & Fambrini, G.L. 2010. The Ediacaran to Cambrian rift system of Southeastern South America: tectonic implications. *Journal of Geology*, **118**, 145–161.
- Almeida, R.P., Santos, M.G.M., Frago-Cesar, A.R., Janikian, L. & Fambrini, G.L. 2012. Recurring extensional and strike-slip tectonics after the Neoproterozoic collisional events in the southern Mantiqueira Province. *Annals of the Brazilian Academy of Sciences*, **84**, 347–376.
- Autin, J., Bellahsen, N., Leroy, S., Husson, L., Beslier, M.O. & d'Acremont, E. 2013. The role of structural inheritance in oblique rifting: Insights from analogue models and application to the Gulf of Aden. *Tectonophysics*, **607**, 51–64.
- Basei, M.A.S., Siga, O., Jr, Masquelin, H., Harara, O.M., Reis Neto, J.M. & Preciozzi, F. 2000. The Dom Feliciano Belt of Brazil and Uruguay and its Foreland Domain the Rio de la Plata Craton: framework, tectonic evolution and correlation with similar provinces of Southwestern Africa. In: Cordani, U. G., Milani, E.J., Thomaz Filho, A. & Campos, D.A. (eds) *Tectonic Evolution of South America. 31st International Geological Congress, Rio de Janeiro, Brazil*, FINEP, Rio de Janeiro 311–334.
- Basei, M.A.S., Frimmel, H.E., Nutman, A.P., Preciozzi, F. & Jacob, J. 2005. The connection between the Neoproterozoic Dom Feliciano (Brazil/Uruguay) and Gariep (Namibia/South Africa) orogenic belts. *Precambrian Research*, **139**, 139–221.
- Basei, M.A.S., Frimmel, H.E., Nutman, A.P. & Preciozzi, F. 2008. West Gondwana amalgamation based on detrital zircon ages from Neoproterozoic Ribeira and Dom Feliciano belts of South America and comparison with coeval sequences from SW Africa. In: Pankhurst, R.J., Trouw, R.A.J., de Brito Neves, B.B. & de Wit, M.J. (eds) *West Gondwana: Pre-Cenozoic Correlations Across the South Atlantic Region*. Geological Society, London, Special Publications, **294**, 239–256. <https://doi.org/10.1144/SP294.13>
- Basei, M.A.S., Peel, E., Sánchez Bettucci, L., Preciozzi, F. & Nutman, A.P. 2011. The basement of the Punta del Este Terrane (Uruguay): an African Mesoproterozoic fragment at the eastern border of the South American Río de la Plata Craton. *International Journal of Earth Sciences*, **100**, 289–304.
- Basei, M.A.S., Sánchez Bettucci, L., Peel, E. & Muzio, R. 2013. Geocronología U–Pb LA-ICP-MS en circones del Complejo Granítico Santa Teresa, Terreno Punta del Este. In: *Proceedings – VII Congreso Uruguayo de Geología*. Sociedad Uruguaya de Geología, Montevideo, 30–31.
- Bense, F.A., Wemmer, K., Löbens, S. & Siegesmund, S. 2014. Fault gouge analyses: K–Ar illite dating, clay mineralogy and tectonic significance – a study from the Sierras Pampeanas, Argentina. *International Journal of Earth Sciences*, **103**, 189–218.
- Bitencourt, M.F. & Nardi, L.V.S. 2000. Tectonic setting and sources of magmatism related to the Southern Brazilian Shear Belt. *Revista Brasileira de Geociências*, **30**, 186–189.
- Campal, N. & Schipilov, A. 1995. The Illescas bluish quartz rapakivi granite (Uruguay – South America): some geological features. In: *Abstracts – Symposium on Rapakivi Granites and Related Rocks*. Academia Brasileira de Ciências, Belem, 18.
- Campal, N. & Schipilov, A. 2005. La Formación Cerros de Aguirre: evidencias de magmatismo Vendiano en el Uruguay. *Latin American Journal of Sedimentology and Basin Analysis*, **12**, 161–174.
- Çemen, I., Catlos, E.J., Göğüs, O. & Özerdem, C. 2006. Postcollisional extensional tectonics and exhumation of the Menderes Massif in the Western Anatolia extended terrane, Turkey. In: Dilek, Y. & Pavlides, S. (eds) *Postcollisional tectonics and magmatism in the Mediterranean region and Asia*. Geological Society of America, Special Papers, **409**, 353–379.
- Cernuschi, F., Dilles, J.H., Kent, A.J.R., Schroer, G., Raab, A.K., Conti, B. & Muzio, R. 2015. Geology, geochemistry and geochronology of the Cretaceous Lascano East Intrusive Complex and magmatic evolution of the Laguna Merin Basin, Uruguay. *Gondwana Research*, **28**, 837–857.
- Chemle, F., Mallmann, G., Bitencourt, M.F. & Kawashita, K. 2012. Time constraints on magmatism along the Major Garcino Shear Zone, southern Brazil: implications for West Gondwana reconstruction. *Gondwana Research*, **22**, 184–199.
- Cingolani, C.A. 2011. The Tandilia System of Argentina as a southern extension of the Río de la Plata Craton: an overview. *International Journal of Earth Sciences*, **100**, 221–242.
- Cingolani, C.A., Basei, M.A.S., Bossi, J., Piñeiro, D. & Uriz, N.J. 2012. U–Pb (LA–ICP–MS) zircon age of the La Paz Granite (Pando Belt, Uruguay): an Upper Neoproterozoic magmatic event in the Río de la Plata Craton. In: *Abstracts – 8th South American Symposium on Isotope Geology, Medellín, Grupo Gemma in Medellín, Colombia*.
- Clauer, N., Zwingmann, H., Liewig, N. & Wendling, R. 2012. Comparative  $^{40}\text{Ar}/^{39}\text{Ar}$  and K–Ar dating of illite-type clay minerals: A tentative explanation for age identities and differences. *Earth-Science Reviews*, **115**, 76–96.
- Cogné, N., Gallagher, K. & Cobbold, P.R. 2011. Post-rift reactivation of the onshore margin of southeast Brazil: evidence from apatite (U–Th)/He and fission-track data. *Earth and Planetary Science Letters*, **309**, 118–130.
- Cogné, N., Gallagher, K., Cobbold, P.R., Ticcomini, C. & Gautheron, C. 2012. Post-breakup tectonics in southeast Brazil from thermochronological data and combined inverse-forward thermal history modelling. *Journal of Geophysical Research B: Solid Earth*, **117**, <https://doi.org/10.1029/2012JB009340>
- Cogné, N., Cobbold, P.R., Riccomini, C. & Gallagher, K. 2013. Tectonic setting of the Taubaté Basin (southeastern Brazil): Insights from regional seismic profiles and outcrop data. *Journal of South American Earth Sciences*, **42**, 194–204.
- Constenius, K.N. 1996. Late Paleogene extensional collapse of the Cordilleran foreland fold and thrust belt. *Geological Society of America Bulletin*, **108**, 20–39.
- de Santa Ana, H. 2004. *Análise Tectono-estratigráfica das Sequências Permotriássica e Jurocretácea da Bacia Chacoparanense Uruguia ('Cuenca Norte')*. PhD thesis, University of São Paulo.
- de Santa Ana, H., Goso, C. & Daners, G. 2006. Cuenca Norte: Estratigrafía del Carbonífero-Pérmico. In: Veroslavsky, G., Ubilla, M. & Martín, S. (eds) *Cuencas Sedimentarias de Uruguay. Geología, Paleontología y Recursos Naturales*. DIRAC, Montevideo, 147–208.
- Demoulin, A., Zarate, M. & Rabassa, J. 2005. Long-term landscape development: a perspective from the southern Buenos Aires ranges of east central Argentina. *Journal of South American Earth Sciences*, **19**, 193–204.
- Dunkl, I., Mikes, T., Simon, K. & von Eynatten, H. 2008. Brief introduction to the Windows program Pepita: data visualization, and reduction, outlier rejection, calculation of trace element ratios and concentrations from LAICPMS data. In: Sylvester, P. (ed.) *Laser Ablation ICP-MS in the Earth Sciences: Current Practices and Outstanding Issues*. Mineralogical Association of Canada, Short Courses, **40**, 334–340.
- Farley, K. A., Wolf, R. A. & Silver, L. T. 1996. The effects of long alpha-stopping distances on (U–Th)/He ages. *Geochimica et Cosmochimica Acta*, **60**, 4223–4229.
- Figueiredo, F.T., Almeida, R.P., Freitas, B.T., Marconato, A., Carrera, S.C. & Turra, B.B. 2015. Tectonic activation, source area stratigraphy and provenance changes in a rift basin: the Early Cretaceous Tucano Basin (NE Brazil). *Basin Research*, **1–13**, <https://doi.org/10.1111/bre.12115>
- Florisbal, L.M.F., Janasi, V.A., Bitencourt, M.F. & Heaman, L.M. 2012. Space–time relation of post-collisional granitic magmatism in Santa Catarina, southern Brazil: U–Pb LAMC-ICP-MS zircon geochronology of coeval mafic–felsic magmatism related to the Major Garcino Shear Zone. *Precambrian Research*, **216–219**, 132–151.
- Flowers, R., Ketcham, R.A., Shuster, D.L. & Farley, K.A. 2009. Apatite (U–Th)/He thermochronometry using a radiation damage accumulation and annealing model. *Geochimica et Cosmochimica Acta*, **73**, 2347–2365.
- Fossen, H. 2010. Extensional tectonics in the North Atlantic Caledonides: a regional view. In: Law, R.D., Butler, R.W.H., Krabbendam, M. & Strachan, R. A. (eds) *Continental Tectonics and Mountain Building: The Legacy of Peach and Horne*. Geological Society, London, Special Publications, **335**, 767–793, <https://doi.org/10.1144/SP335.31>
- Fossen, H., Khani, H.F., Faleide, J.I., Ksienzyk, A.K. & Dunlap, W.J. 2016. Post-Caledonian extension in the West Norway–northern North Sea region: the role



- of structural inheritance. In: Childs, C., Holdsworth, R.E., Jackson, C.A.-L., Manzocchi, T., Walsh, J.J. & Yielding, G. (eds) *The Geometry and Growth of Normal Faults*. Geological Society, London, Special Publications, **439**, <https://doi.org/10.1144/SP439.6>
- Foster, D.A., Goscombe, B.D. & Gray, D.R. 2009. Rapid exhumation of deep crust in an obliquely convergent orogeny: the Kaoko Belt of the Damara Orogen. *Tectonics*, **28**, <https://doi.org/10.1029/2008TC002317>
- Franco-Magalhães, A.O.B., Hackspacher, P.C., Glasmacher, U.A. & Saad, A.R. 2010. Rift to post-rift evolution of a 'passive' continental margin: the Ponta Grossa Arch, SE Brazil. *International Journal of Earth Sciences*, **99**, 1599–1613.
- Franco-Magalhães, A.O.B., Cuglieri, M.A.A., Hackspacher, P.C. & Saad, A.R. 2014. Long-term landscape evolution and post-rift reactivation in the southeastern Brazilian passive continental margin: Taubaté Basin. *International Journal of Earth Sciences*, **103**, 441–453.
- Fuhrmann, U., Lippolt, H.J. & Hess, J.C. 1987. Examination of some proposed K–Ar standards:  $^{40}\text{Ar}/^{39}\text{Ar}$  analyses and conventional K–Ar data. *Chemical Geology*, **66**, 41–51.
- Goscombe, B., Gray, D., Armstrong, R., Foster, D.A. & Vogl, J. 2005. Event geochronology of the Pan-African Kaoko Belt, Namibia. *Precambrian Research*, **140**, 103.e1–103.e41.
- Gray, D. R., Foster, D. A., Goscombe, B., Passchier, C.W. & Trouw, R. A. J. 2006.  $^{40}\text{Ar}/^{39}\text{Ar}$  thermochronology of the Pan-African Damara Orogen, Namibia with implications for tectonothermal and geodynamic evolution. *Precambrian Research*, **150**, 49–72.
- Guenther, W.R., Reiners, P.W., Ketcham, R.A., Nasdala, L. & Giester, G. 2013. Helium diffusion in natural zircon: radiation damage, anisotropy, and the interpretation of zircon (U–Th)/He thermochronology. *American Journal of Science*, **313**, 145–198.
- Guenther, W.R., Reiners, P.W., DeCelles, P.G. & Kendall, J. 2015. Sevier Belt exhumation in central Utah constrained from complex zircon (U–Th)/He data sets: Radiation damage and He inheritance effects on partially reset detrital zircons. *Geological Society of America Bulletin*, **127**, <https://doi.org/10.1130/B31032.1>
- Hackspacher, P.C., Ribeiro, L.F.B., Ribeiro, M.C.S., Fetter, A.H., Hadler Neto, J. C., Tello Saenz, C.A. & Dantas, E.L. 2004. Consolidation and break-up of the South American platform in southeastern Brazil: tectonothermal and denudation histories. *Gondwana Research*, **1**, 91–101.
- Haines, S.H. & van der Pluijm, B.A. 2008. Clay quantification and Ar–Ar dating of synthetic and natural gouge: application to the Miocene Sierra Mazatan detachment fault, Sonora, Mexico. *Journal of Structural Geology*, **30**, 525–538.
- Harrison, T.M., Célérier, J., Aikman, A.B., Hermann, J. & Heizler, M.T. 2009. Diffusion of  $^{40}\text{Ar}$  in muscovite. *Geochimica et Cosmochimica Acta*, **73**, 1039–1051.
- Hartmann, L.A., Campal, N., Santos, J.O.S., McNaughton, N.J., Bossi, J., Schipilov, A. & Lafon, J.-M. 2001. Archean crust in the Río de la Plata Craton, Uruguay – SHRIMP U–Pb zircon reconnaissance geochronology. *Journal of South American Earth Sciences*, **4**, 557–570.
- Hartmann, L.A., Santos, J.O.S., Bossi, J., Campal, N., Schipilov, A. & McNaughton, N.J. 2002. Zircon and titanite U–Pb SHRIMP geochronology of Neoproterozoic felsic magmatism on the eastern border of the Río de la Plata Craton, Uruguay. *Journal of South American Earth Sciences*, **15**, 229–236.
- Hartmann, L.A., Liu, D., Wang, Y., Massonne, H.J. & dos Santos, J. 2008. Protolith age of Santa Maria Chico Granulites dated on zircons from an associated amphibolite-facies granulodiorite in southernmost Brazil. *Annals of the Brazilian Academy of Sciences*, **80**, 543–551.
- Henza, A.A., Withjack, M.O. & Schlichte, R.W. 2011. How do the properties of a pre-existing normal-fault population influence fault development during a subsequent phase of extension? *Journal of Structural Geology*, **33**, 1312–1324.
- Hiruma, S.T., Riccomini, C., Modenesi-Gauttieri, M.C., Hackspacher, P.C., Hadler Neto, J.C. & Franco-Magalhães, A.O.B. 2010. Denudation history of the Bocaina Plateau, Serra do Mar, Southeastern Brazil: relationships to Gondwana breakup and passive margin development. *Gondwana Research*, **18**, 674–687.
- Hurter, S.J. & Pollack, H.N. 1994. Effect of the Cretaceous Serra Geral igneous event on the temperatures and heat flow of the Paraná Basin, southern Brazil. *Basin Research*, **6**, 239–244.
- Janasi, V.A., Freitas, V.A. & Heaman, L.H. 2011. The onset of flood basalt volcanism, Northern Paraná Basin, Brazil: A precise U–Pb baddeleyite/zircon age for a Chapecó-type dacite. *Earth and Planetary Science Letters*, **302**, 147–153.
- Jelinek, A.R., Chemale, F.C., Jr, van der Beek, P.A., Guadagnin, F., Cupertino, J. A. & Viana, A. 2014. Denudation history and landscape evolution of the northern East-Brazilian continental margin from apatite fission-track thermochronology. *Journal of South American Earth Sciences*, **54**, 158–181.
- Karl, M., Glasmacher, U.A., Kollenz, S., Franco-Magalhães, A.O.B., Stockli, D. F. & Hackspacher, P.C. 2013. Evolution of the South Atlantic passive continental margin in southern Brazil derived from zircon and apatite (U–Th–Sm)/He and fission-track data. *Tectonophysics*, **604**, 224–244.
- Ketcham, R.A. 2005. Forward and inverse modeling of low-temperature thermochronometry data. In: Reiners, P.W. & Ehlers, T.A. (eds) *Low-temperature Thermochronology: Techniques, Interpretations, and Applications*. Mineralogical Society of America and Geochemical Society, Reviews in Mineralogy and Geochemistry, **58**, 275–314.
- Ketcham, R.A., Gautheron, C. & Tassan-Got, L. 2011. Accounting for long alpha-particle stopping distances in (U–Th–Sm)/He geochronology: Refinement of the baseline case. *Geochimica et Cosmochimica Acta*, **75**, 7779–7791.
- Kleiman, L.E. & Japas, M.S. 2009. The Choiyoi volcanic province at 34°S–36°S (San Rafael, Mendoza, Argentina): Implications for the Late Paleozoic evolution of the southwestern margin of Gondwana. *Tectonophysics*, **473**, 283–299.
- Kollenz, S. 2015. *Long-term landscape evolution, cooling and exhumation history of the South American passive continental margin in NE Argentina and SW Uruguay*. PhD thesis, Ruprecht-Karls-Universität Heidelberg.
- Ksienzyk, A.K., Wemmer, K. et al. 2016. Post-Caledonian brittle deformation in the Bergen area, West Norway: results from K–Ar illite fault gouge dating. *Norwegian Journal of Geology*, **96**, 1–25.
- Kübler, B. 1967. La cristallinité de l'illite et les zones tout à fait supérieures du métamorphisme. *Etages Tectonique, Colloque de Neuchâtel*, University Neuchâtel, à la Baconnière, Suisse, 105–121.
- Lenz, C., Fernandes, L.A.D., McNaughton, N.J., Porcher, C.C. & Masquelin, H. 2011. U–Pb SHRIMP ages for the Cerro Bori Orthogneisses, Dom Feliciano Belt in Uruguay: Evidences of a ~800 Ma magmatic and a ~650 Ma metamorphic event. *Precambrian Research*, **185**, 149–163.
- Löbens, S., Bense, F.A., Wemmer, K., Dunkl, I., Costa, C.H., Layer, P. & Siegesmund, S. 2011. Exhumation and uplift of the Sierras Pampeanas: preliminary implications from K–Ar fault gouge dating and low-T thermochronology in the Sierra de Comechingones (Argentina). *International Journal of Earth Sciences*, **100**, 671–694.
- López-Gamundi, O.R. & Rossello E.A. 1993. Devonian–Carboniferous unconformity in Argentina and its relation to the Eo-Hercynian orogeny in southern South America. *Geologische Rundschau*, **82**, 136–147.
- Mallmann, G., Chemale, F., Jr, Ávila, J.N., Kawashita, K. & Armstrong, R.A. 2007. Isotope geochemistry and geochronology of the Nico Pérez Terrane, Río de la Plata Craton, Uruguay. *Gondwana Research*, **12**, 489–508.
- Masquelin, H., Aifa, T., Muzio, R., Hallot, E., Veroslavsky, G. & Bonneville, L. 2009. The Cuaró Mesozoic doleritic dyke swarm, southern Paraná Basin, Uruguay: Examples of superimposed magnetic fabrics? *Comptes Rendus Géoscience*, **341**, 1003–1015.
- Meisling, K.E., Cobbold, P.R. & Mount, V.S. 2001. Segmentation of an obliquely rifted margin, Campos and Santos basins, southeastern Brazil. *AAPG Bulletin*, **85**, 1903–1924.
- Milani, E. & Davison, I. 1988. Basement control and transfer tectonics in the Recôncavo–Tucano–Jatobá Rift, Northeast Brazil. *Tectonophysics*, **154**, 41–70.
- Milani, E.J., Melo, J.H.G., Souza, P.A., Fernandes, L.A. & França, A.B. 2007. Bacia do Paraná. In: Milani, E.J., Rangel, H.D., Bueno, G.V., Stica, J.M., Winter, W.R., Caixeta, J.M. & Pessoa Neto, O.C. (eds) *Bacias Sedimentares Brasileiras – Cartas Estratigráficas*. Boletim de Geociências da Petrobras, **15**, Rio de Janeiro, 265–287.
- Morley, C.K. 1995. Developments in the structural geology of rifts over the last decade and their impact on hydrocarbon exploration. In: Lambiasi, J. (ed.) *Hydrocarbon Habitat of Rift Basins*. Geological Society, London, Special Publications, **80**, 1–32, <https://doi.org/10.1144/GSL.SP.1995.080.01.01>
- Morley, C.K., Haranya, C., Phoosongsee, W., Pongwapee, S., Kornsawan, A. & Wonganan, N. 2004. Activation of rift oblique and rift parallel pre-existing fabrics during extension and their effect on deformation style: examples from the rifts of Thailand. *Journal of Structural Geology*, **26**, 1803–1829.
- Murray, K.E., Reiners, P.W. & Thomson, S.N. 2016. Rapid Pliocene–Pleistocene erosion of the central Colorado plateau documented by apatite thermochronology from the Henry Mountains. *Geology*, **44**, 483–486.
- Nasdala, L., Wenzel, M., Vavra, G., Irmer, G., Wenzel, T. & Kober, B. 2001. Metamictisation of natural zircon: accumulation versus thermal annealing of radioactivity-induced damage. *Contributions to Mineralogy and Petrology*, **141**, 125–144.
- Oliveira, C.H.E., Jelinek, A.R., Chemale, F., Jr & Bernet, M. 2015. Evidence of post-Gondwana breakup in Southern Brazilian Shield: Insights from apatite and zircon fission track thermochronology. *Tectonophysics*, **666**, 173–187.
- Oriolo, S., Oyhantçabal, P., Heidebach, F., Wemmer, K. & Siegesmund, S. 2015. Structural evolution of the Sarandí del Yí Shear Zone: kinematics, deformation conditions and tectonic significance. *International Journal of Earth Sciences*, **104**, 1759–1777.
- Oriolo, S., Oyhantçabal, P., Basei, M.A.S., Wemmer, K. & Siegesmund, S. 2016a. The Nico Pérez Terrane (Uruguay): From Archean crustal growth and connections with the Congo Craton to late Neoproterozoic accretion to the Río de la Plata Craton. *Precambrian Research*, **280**, 147–160.
- Oriolo, S., Oyhantçabal, P. et al. 2016b. Shear zone evolution and timing of deformation in the Neoproterozoic transpressional Dom Feliciano Belt, Uruguay. *Journal of Structural Geology*, **92**, 59–78.
- Oriolo, S., Oyhantçabal, P. et al. 2016c. Timing of deformation in the Sarandí del Yí Shear Zone, Uruguay: Implications for the amalgamation of western Gondwana during the Neoproterozoic Brasiliano–Pan-African Orogeny. *Tectonics*, **35**, <https://doi.org/10.1002/2015TC004052>
- Orme, D.A., Guenther, W.R., Laskowski, A.K. & Reiners, P.W. 2016. Long-term tectonothermal history of Laramide basement from zircon–He age–eU correlations. *Earth and Planetary Science Letters*, **453**, 119–130.
- Oyhantçabal, P. 2005. *The Sierra Ballena shear zone: kinematics, timing and its significance for the geotectonic evolution of southeast Uruguay*. PhD dissertation, Georg-August-Universität Göttingen.

- Oyhantçabal, P., Siegesmund, S., Wemmer, K., Robert, F. & Lyster, P. 2007. Post-collisional transition from calc-alkaline to alkaline magmatism during transcurrent deformation in the southernmost Dom Feliciano Belt (Braziliano–Pan-African, Uruguay). *Lithos*, **98**, 141–159.
- Oyhantçabal, P., Siegesmund, S., Wemmer, K. & Lyster, P. 2009a. The Sierra Ballena Shear Zone in the southernmost Dom Feliciano Belt (Uruguay): evolution, kinematics, and deformation conditions. *International Journal of Earth Sciences*, **99**, <https://doi.org/10.1007/s00531-009-0453-1>
- Oyhantçabal, P., Siegesmund, S., Wemmer, K., Presnyakov, S. & Lyster, P. 2009b. Geochronological constraints on the evolution of the southern Dom Feliciano Belt (Uruguay). *Journal of the Geological Society, London*, **166**, 1075–1084, <https://doi.org/10.1144/0016-76492008-122>
- Oyhantçabal, P., Siegesmund, S. & Wemmer, K. 2011a. The Río de la Plata Craton: a review of units, boundaries, ages and isotopic signature. *International Journal of Earth Sciences*, **100**, 201–220.
- Oyhantçabal, P., Siegesmund, S., Wemmer, K. & Passchier, C.W. 2011b. The transpressional connection between Dom Feliciano and Kaoko Belts at 580–550 Ma. *International Journal of Earth Sciences*, **100**, 379–390.
- Oyhantçabal, P., Wegner-Eimer, M., Wemmer, K., Schulz, B., Frei, R. & Siegesmund, S. 2012. Paleo- and Neoproterozoic magmatic and tectonometamorphic evolution of the Isla Cristalina de Rivera (Nico Pérez Terrane, Uruguay). *International Journal of Earth Sciences*, **101**, 1745–1762.
- Panario, D., Gutiérrez, O., Sánchez-Bettucci, L., Peel, E., Oyhantçabal, P. & Rabassa, J. 2014. Ancient landscapes of Uruguay. In: Rabassa, J. & Ollier, C. (eds) *Gondwana Landscapes in Southern South America*. Springer, Dordrecht, 161–199.
- Pángaro, F., Ramos, V.A. & Pazos, P.J. 2015. The Hesperides Basin: a continental-scale upper Palaeozoic to Triassic basin in southern Gondwana. *Basin Research*, **1**–27, <https://doi.org/10.1111/bre.12126>
- Passarelli, C.R., Basei, M.A.S., Siga, O., Jr, McReath, I. & Campos Neto, M.C. 2010. Deformation and geochronology of syntectonic granitoids emplaced in the Major Gercino Shear Zone, southeastern South America. *Gondwana Research*, **17**, 688–703.
- Peron-Pinvidic, G., Manatschal, G. & Osmundsen, P.T. 2013. Structural comparison of archetypal Atlantic rifted margins: A review of observations and concepts. *Marine and Petroleum Geology*, **13**, 21–47.
- Philipp, R.P. & Machado, R. 2005. The Neoproterozoic to Cambrian granitic magmatism of the Pelotas Batholith, southern Brazil. *Journal of South American Earth Sciences*, **19**, 461–478.
- Purdy, J. W. & Jäger, E. 1976. K–Ar ages on rock-forming minerals from the Central Alps. *Memorie degli Istituti di Geologia e Mineralogia dell'Università di Padova*, **30**, 1–31.
- Rapela, C.W., Fanning, C.M., Casquet, C., Pankhurst, R.J., Spalletti, L., Poiré, D. & Baldo, E.G. 2011. The Río de la Plata Craton and the adjoining Pan-African/Brazilian terranes: their origins and incorporation into south-west Gondwana. *Gondwana Research*, **20**, 673–690.
- Renne, P.R., Ernesto, M., Pacca, I.G., Coe, R.S., Glen, J.M., Prévot, M. & Perrin, M. 1992. The age of Paraná flood volcanism, rifting of Gondwanaland, and the Jurassic–Cretaceous boundary. *Science*, **258**, 975–979.
- Riccomini, C., Sant'Anna, L.G. & Ferrari, A.L. 2004. Evolução geológica do Rift Continental do Sudeste do Brasil. In: Mantesso-Neto, V., Bartorelli, A., Carneiro, C.D.R. & Brito-Neves, B.D. (eds) *Geologia do Continente Sul-Americano: Evolução da Obra de Fernando Flávio Marques de Almeida*. Beca, São Paulo, 383–405.
- Rocha Campos, A.C., Basei, M.A.S., Nutman, A.P. & Santos, P.R. dos 2006. SHRIMP U–Pb zircon geochronological calibration of the late Paleozoic supersequence, Paraná Basin, Brazil. In: Bossi, J.L. (ed.) *Quinto Simposio Sudamericano de Geologia Isotópica*, Actas. Idea Grafica, Punta del Este, Uruguay, 322–325.
- Rossello, E.A., de Santa Ana, H. & Veroslavsky, G. 2000. El Lineamiento Santa Lucía–Aiguá–Merín (Uruguay): Un corredor tectónico extensivo y transcurrente dextral precursor de la apertura Atlántica. *Revista Brasileira de Geociências*, **30**, 749–756.
- Rossello, E.A., Veroslavsky, G., Masquelin, H. & de Santa Ana, H. 2007. El corredor Juro-Cretácico Santa Lucía–Aiguá–Merín (Uruguay): cinemática transcurrente dextral y controles preexistentes. *Revista de la Asociación Geológica Argentina*, **62**, 92–104.
- Rostirolla, S.P., Assine, M.L., Fernandes, L.A. & Artur, P.C. 2000. Reativação de paleolineamentos durante a evolução da Bacia do Paraná – o exemplo do alto estrutural de Quatiguá. *Revista Brasileira de Geociências*, **30**, 639–648.
- Salomon, E., Koehn, D., Passchier, C., Hackspacher, P.C. & Glasmacher, U.A. 2015. Contrasting stress fields on correlating margins of the South Atlantic. *Gondwana Research*, **28**, 1152–1167.
- Sánchez Bettucci, L., Oyhantçabal, P., Loureiro, J., Ramos, V.A., Preciozzi, F. & Basei, M.A.S. 2004. Mineralizations of the Lavaljeja Group (Uruguay), a probable Neoproterozoic volcano-sedimentary sequence. *Gondwana Research*, **6**, 89–105.
- Sánchez Bettucci, L., Masquelin, E., Peel, E., Oyhantçabal, P., Muzio, R., Ledesma, J.J. & Preciozzi, F. 2010. Comment on Provenance of the Arroyo del Soldado Group (Ediacaran to Cambrian, Uruguay): Implications for the paleogeographic evolution of southwestern Gondwana, by Blanco *et al.* 2009 [Precambrian Research, 171, 57–63]. *Precambrian Research*, **180**, 328–333.
- Sato, A.M., Llambías, E.J., Basei, M.A.S. & Castro, C.E. 2015. Three stages in the Late Paleozoic to Triassic magmatism of southwestern Gondwana, and the relationships with the volcanogenic events in coeval basins. *Journal of South American Earth Sciences*, **63**, 48–69.
- Schumacher, E. 1975. Herstellung von 99.9997%  $^{38}\text{Ar}$  für die  $^{40}\text{K}/^{40}\text{Ar}$  Geochronologie. *Geochronologia Chimica*, **24**, 441–442.
- Silva, Z.C.C. & Cornford, C. 1985. The kerogen type, depositional environment and maturity of the Irati Shale, Upper Permian of Paraná Basin, southern Brazil. *Organic Geochemistry*, **8**, 399–411.
- Soto, M., Morales, E., Veroslavsky, G., de Santa Ana, H., Ucha, N. & Rodríguez, P. 2011. The continental margin of Uruguay: Crustal architecture and segmentation. *Marine and Petroleum Geology*, **28**, 1676–1689.
- Souza, I.V.A.F., Mendonça Filho, J.G. & Menezes, T.R. 2008. Avaliação do efeito térmico das intrusivas ígneas em um horizonte potencialmente gerador da Bacia do Paraná: Formação Irati. *Revista Brasileira de Geociências*, **38**, 138–148.
- Steenken, A., López de Luci, M.G., Dopico, C.M., Drobe, M., Wemmer, K. & Siegesmund, S. 2011. The Neoproterozoic–early Paleozoic metamorphic and magmatic evolution of the Eastern Sierras Pampeanas: An overview. *International Journal of Earth Sciences*, **100**, 465–488.
- Strugale, M., Rostirolla, S.P., Mancini, F., Portela Filho, C.V., Ferreira, F.J.F. & Freitas, R.C. 2007. Structural framework and Mesozoic–Cenozoic evolution of Ponta Grossa Arch, Paraná Basin, southern Brazil. *Journal of South American Earth Sciences*, **24**, 203–227.
- Tagami, T. 2012. Thermochronological investigation of fault zones. *Tectonophysics*, **538–540**, 67–85.
- Tello Saenz, C.A., Hackspacher, P.C., Hadler, N.J.C., Iunes, P.J., Guedes, S., Paulo, S.R. & Ribeiro, L.F.B. 2003. Recognition of Cretaceous, Paleocene and Neogene tectonic reactivation, through apatite fission-track analysis in Precambrian areas of the Southeast Brazil: Association with the South Atlantic Ocean opening. *Journal of South American Earth Sciences*, **15**, 137–142.
- Torgersen, E., Viola, G., Zwingmann, H. & Henderson, I.H.C. 2015. Inclined K–Ar illite age spectra in brittle fault gouges: effects of fault reactivation and wall-rock contamination. *Terra Nova*, **27**, 106–113.
- Tremblay, A., Roden-Tice, M.K., Brandt, J.A. & Megan, T.W. 2013. Mesozoic fault reactivation along the St. Lawrence rift system, eastern Canada: Thermochronological evidence from apatite fission-track dating. *Geological Society of America Bulletin*, **125**, 794–810.
- Uriz, N.J., Cingolani, C.A., Basei, M.A.S., Blanco, G., Abre, P., Portillo, N.S. & Siccardi, A. 2016. Provenance and paleogeography of the Devonian Durazno Group, southern Paraná Basin in Uruguay. *Journal of South American Earth Sciences*, **66**, 248–267.
- van der Pluijm, B.A., Hall, C.M., Vrolijk, P.J., Pevear, D.R. & Covey, M.C. 2001. The dating of shallow faults in the Earth's crust. *Nature*, **412**, 172–175.
- von Gosen, W., Buggisch, W. & Dimieri, L.V. 1990. Structural and metamorphic evolution of the Sierras Australes (Buenos Aires Province/Argentina). *Geologische Rundschau*, **79**, 797–821.
- Wemmer, K. 1991. K/Ar-Altersdatierungsmöglichkeiten für retrograde Deformationsprozesse im spröden und duktilen Bereich – Beispiele aus der KTB Vorbohrung (Oberpfalz) und dem Bereich der Insubrischen Linie (N-Italien). *Göttinger Arbeiten zur Geologie und Paläontologie*, **51**, 1–61.
- Wolff, R., Dunkl, I., Kiesselbach, G., Wemmer, K. & Siegesmund, S. 2012. Thermochronological constraints on the multiphase exhumation history of the Ivrea–Verbano Zone of the Southern Alps. *Tectonophysics*, **579**, 104–117.
- Zalán, P.V., Wolff, S. *et al.* 1990. The Paraná Basin, Brazil. In: Leighton, M.W., Kolata, D.R., Oltz, D.F. & Eidel, J.J. (eds) *Interior Cratonic Basins*. AAPG Memoirs, **51**, 681–708.
- Zerfass, H., Chemale, F., Jr, Schultz, C.L. & Lavina, E. 2004. Tectonics and sedimentation in southern South America during Triassic. *Sedimentary Geology*, **166**, 265–292.
- Zwingmann, H., Mancktelow, N., Antognini, M. & Lucchini, R. 2010. Dating of shallow faults: new constraints from the AlpTransit tunnel site (Switzerland). *Geology*, **38**, 487–490.